DSE/2538-4

DEVELOPMENT OF A THIN FILM POLYCRYSTALLINE SOLAR CELL FOR LARGE SCALE TERRESTRIAL USE

Final Report, July 1, 1976—June 30, 1977

November 1977

MASTER

Work Performed Under Contract No. EX-76-C-01-2538

Institute of Energy Conversion
University of Delaware
Newark, Delaware

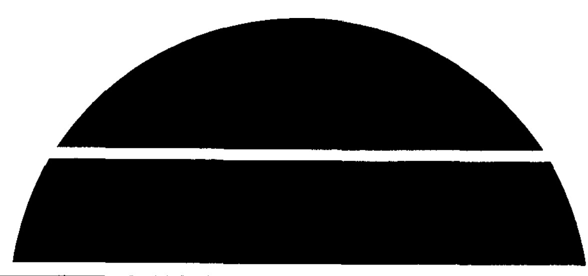

U.S. Department of Energy

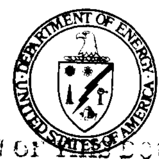

Solar Energy

DISTRIBUTION OF THIS DOCUMENT IS UNLIMITED

DISCLAIMER

This report was prepared as an account of work sponsored by an agency of the United States Government. Neither the United States Government nor any agency thereof, nor any of their employees, makes any warranty, express or implied, or assumes any legal liability or responsibility for the accuracy, completeness, or usefulness of any information, apparatus, product, or process disclosed, or represents that its use would not infringe privately owned rights. Reference herein to any specific commercial product, process, or service by trade name, trademark, manufacturer, or otherwise does not necessarily constitute or imply its endorsement, recommendation, or favoring by the United States Government or any agency thereof. The views and opinions of authors expressed herein do not necessarily state or reflect those of the United States Government or any agency thereof.

DISCLAIMER

Portions of this document may be illegible in electronic image products. Images are produced from the best available original document.

NOTICE

This report was prepared as an account of work sponsored by the United States Government. Neither the United States nor the United States Department of Energy, nor any of their employees, nor any of their contractors, subcontractors, or their employees, makes any warranty, express or implied, or assumes any legal liability or responsibility for the accuracy, completeness or usefulness of any information, apparatus, product or process disclosed, or represents that its use would not infringe privately owned rights.

This report has been reproduced directly from the best available copy.

Available from the National Technical Information Service, U. S. Department of Commerce, Springfield, Virginia 22161.

Price: Paper Copy $5.25
Microfiche $3.00

DSE/2538-4
Distribution Category UC-63e

DEVELOPMENT OF A THIN FILM POLYCRYSTALLINE SOLAR CELL FOR LARGE SCALE TERRESTRIAL USE

Final Report

July 1, 1976 - June 30, 1977

E(49-18)-2538

November 1977

INSTITUTE OF ENERGY CONVERSION

UNIVERSITY OF DELAWARE
NEWARK, DELAWARE 19711

NOTICE

This report was prepared as an account of work sponsored by the United States Government. Neither the United States nor the United States Department of Energy, nor any of their employees, nor any of their contractors, subcontractors, or their employees, makes any warranty, express or implied, or assumes any legal liability or responsibility for the accuracy, completeness or usefulness of any information, apparatus, product or process disclosed, or represents that its use would not infringe privately owned rights.

Supported by the Energy Research and Development Administration

Report: E(49-18)-2538 FR77

DISTR[illegible]

BIBLIOGRAPHIC DATA SHEET

1. Report No. E(49-18)-2538 FR77

2.

3. Recipient's Accession No.

4. Title and Subtitle
Development of a Thin Film Polycrystalline Solar Cell for Large Scale Terrestrial Use

5. Report Date
November 1977

6.

7. Author(s)

8. Performing Organization Rept. No.

9. Performing Organization Name and Address
Institute of Energy Conversion
University of Delaware
Newark, Delaware 19711

10. Project/Task/Work Unit No.

11. Contract/Grant No.
E(49-18)-2538

12. Sponsoring Organization Name and Address
Department of Energy
Division of Solar Energy
20 Massachusetts Avenue, N. W.
Washington, DC 20545

13. Type of Report & Period Covered
Final
7/1/76 - 6/30/77

14.

15. Supplementary Notes

16. Abstracts

A complete quantitative analysis of all the factors influencing cell efficiency has been conducted using as input direct material, electronic and optical measurements. The output of the analysis has been used to direct a systematic cell improvement program which has resulted in the practical achievement of anticipated cell efficiencies. During the program year the maximum CdS/Cu_2S cell efficiency was increased from an initial value of 7.64% to 8.55%. Short circuit currents under AM1 illumination exceeded 26 mA/cm^2. Excellent reproducibility has been maintained; the group of 47 cells containing the 8.55% cell showed only one failure and over half the cells had efficiencies that would exceed 7.5% in sunlight. Individual cell parameters show conclusively that the cell design that to date has given an efficiency of 8.55% is in fact capable of reaching 9.0%. The design changes necessary to produce cells above 10% have been identified. Applying the same analysis driven development to $(CdZn)S/Cu_2S$ cells has resulted in efficiencies up to 6.29% largely as a result of increasing short circuit currents from the initial level of $\sim$ 5 mA/cm^2 to > 14 mA/cm^2 for open circuit voltages between 0.60 and 0.68 V. Further development of this cell is expected to yield ultimate cell efficiencies of close to 15%.

17. Key Words and Document Analysis. 17a. Descriptors

Photovoltaic Conversion

CdS Solar Cells

Heterojunctions

17b. Identifiers/Open-Ended Terms

Solar Energy

17c. COSATI Field/Group

18. Availability Statement

19. Security Class (This Report) UNCLASSIFIED

20. Security Class (This Page) UNCLASSIFIED

21. No. of Pages

22. Price

FORM NTIS-35 (REV. 3-72)

USCOMM-DC 14952-P72

Abstract

A complete quantitative analysis of all the factors influencing cell efficiency has been conducted using as input direct material, electronic and optical measurements. The output of the analysis has been used to direct a systematic cell improvement program which has resulted in the practical achievement of anticipated cell efficiencies. During the program year the maximum CdS/Cu_2S cell efficiency was increased from an initial value of 7.64% to 8.55%. Short circuit currents under AM1 illumination exceeded 26 mA/cm^2. Excellent reproducibility has been maintained; the group of 47 cells containing the 8.55% cell showed only one failure and over half the cells had efficiencies that would exceed 7.5% in sunlight. Individual cell parameters show conclusively that the cell design that to date has given an efficiency of 8.55% is in fact capable of reaching 9.0%. The design changes necessary to produce cells above 10% have been identified. Applying the same analysis driven development to $(CdZn)S/Cu_2S$ cells has resulted in efficiencies up to 6.29% largely as a result of increasing short circuit currents from the initial level of $\sim$ 5 mA/cm^2 to > 14 mA/cm^2 for open circuit voltages between 0.60 and 0.68 V. Further development of this cell is expected to yield ultimate cell efficiencies of close to 15%.

Final Report, July 1, 1976 - June 30, 1977

2. Table of Contents

	Page
Bibliographic Data Sheet	ii
1. Abstract	1
2. Table of Contents	3
List of Illustrations	4
List of Tables	5
3. Summary	6
4. Introduction	10
4.1 Objectives	10
4.2 Approach and Key Methods	11
5. Cell Production and Analysis	12
5.1 Development of CdS/Cu_2S cells	12
5.2 Development of $(CdZn)S/Cu_2S$ Cells	12
5.3 Electro-Optical and Theoretical Analysis	16
6. References	34

APPENDIX A. List of Research Contributors
B. Design Analysis of the Thin-Film CdS-Cu_2S Solar Cell
C. Progress in the Development of High Efficiency Thin Film Cadmium Sulfide Solar Cells
D. Formation and Characterization of $(CdZn)S$ Films and $(CdZn)S/Cu_2S$ Heterojunctions
E. Reports and Publications

List of Figures

Figure 1. Chronological development of short circuit current for both CdS/Cu_2S and $(CdZn)S/Cu_2S$ cells.

Figure 2. Chronological development of power conversion efficiency for both CdS/Cu_2S and $(CdZn)S/Cu_2S$ cells.

Figure 3. Histogram of cell efficiencies for 47 cells.

Figure 4. Surface structure of textured (etched) and as deposited CdS.

Figure 5. Dependence of light sensitive shunt resistance on short circuit current.

List of Tables

Table 1. Performance figures for 47 cells made on textured CdS with evaporated grids and a single layer SiO anti-reflection coating.

Table 2. Influence of heat treatment on the capacitance of CdS/Cu_2S and $(CdZn)S/Cu_2S$ cells.

Table 3. Influence of CdS resistivity on open circuit voltage.

Table 4. Influence of heat treatment and surface texture on the apparent width of the depletion region.

Table 5. Influence of various illumination spectra on cell behavior.

Table 6. Variation of apparent shunt resistance with illumination.

3. Summary

When the NSF program[1] was completed in June 1976, the highest CdS/Cu_2S cell efficiency achieved was 7.64%. During the course of this ERDA program, the maximum efficiency measured in sunlight was 8.55%. The maximum short circuit current measured in sunlight was 0.26 mA/mW and simulator tests indicated that the cell design was capable of currents well in excess of 26 mA/cm^2 at 100 mW/cm^2.

Development of cells based on $(CdZn)S/Cu_2S$ has resulted in cell efficiencies of up to 6.29% and open circuit voltages as high as 0.7 volts. Steady progress has been made in raising the short circuit currents from the initial values of $\sim$ 5 mA/cm^2 to values in excess of 14 mA/cm^2 for open circuit voltages between 0.60 and 0.68 V.

The loss minimization analysis for CdS/Cu_2S and $(CdZn)S/Cu_2S$ thin film solar cells has been refined and published (Appendix B). Cell development has been directed by the application of this analysis and as a result systematic and anticipated increases in cell conversion efficiency have been made.

During the final quarter, 47 CdS/Cu_2S cells were made with an evaporated grid of 96% transmission and a single SiO anti-reflection layer. The highest efficiency achieved was 8.55% in sunlight, over half the cells would exceed 7.5% efficiency in sunlight and only one cell was a failure.

Control and reproducibility of the (CdZn)S deposition has improved and resistivities of $\sim$ 1 Ω cm have been achieved at 10% zinc content and should shortly be possible up to 20% zinc content.

The improvement in short circuit current and efficiency for both types of cells is shown in Figures 1 and 2. The substantial improvement during the contract year is evident for both types of cells.

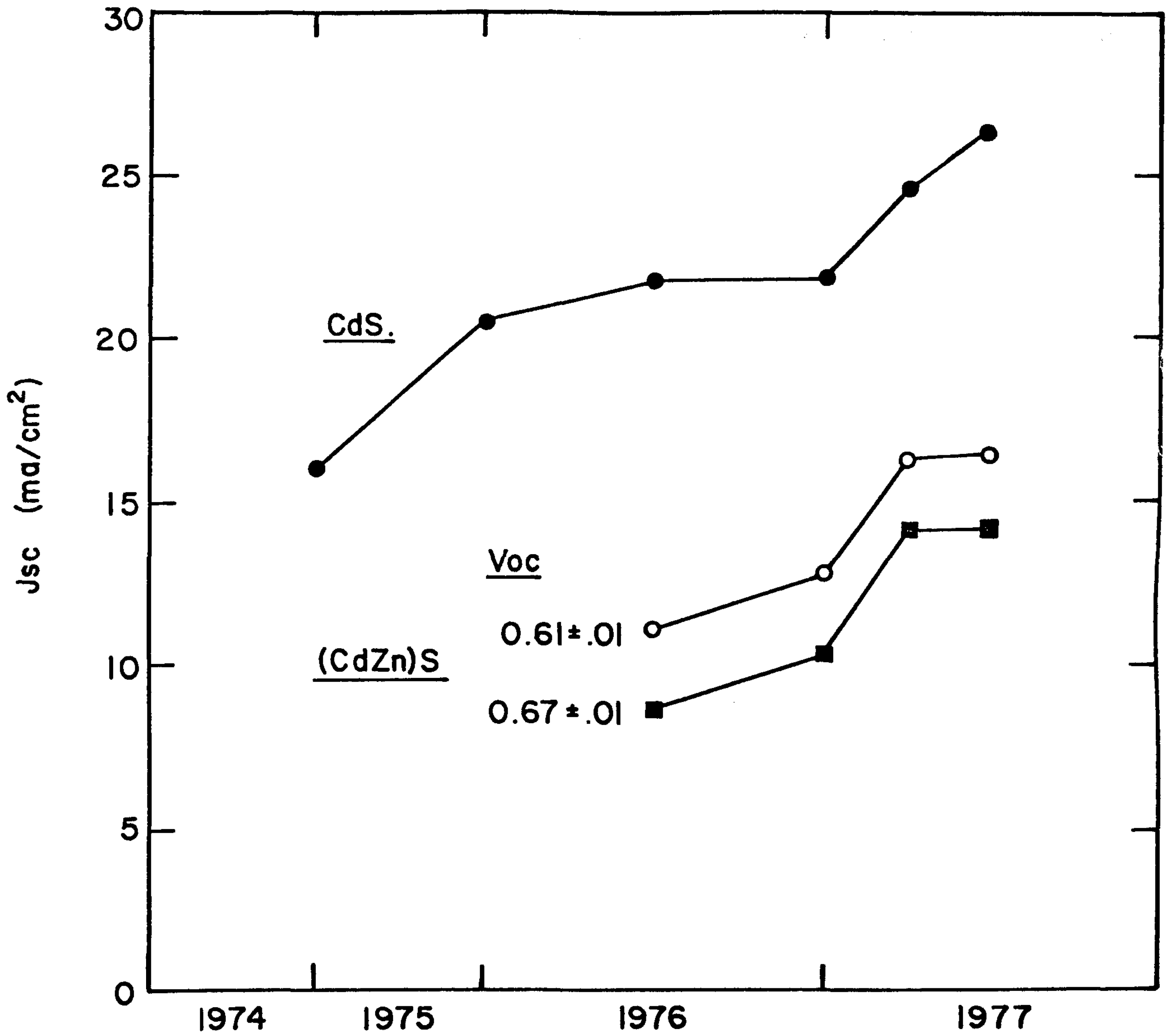

Figure 1. Chronological development of short circuit current for both CdS/Cu_2S and $(CdZn)S/Cu_2S$ cells.

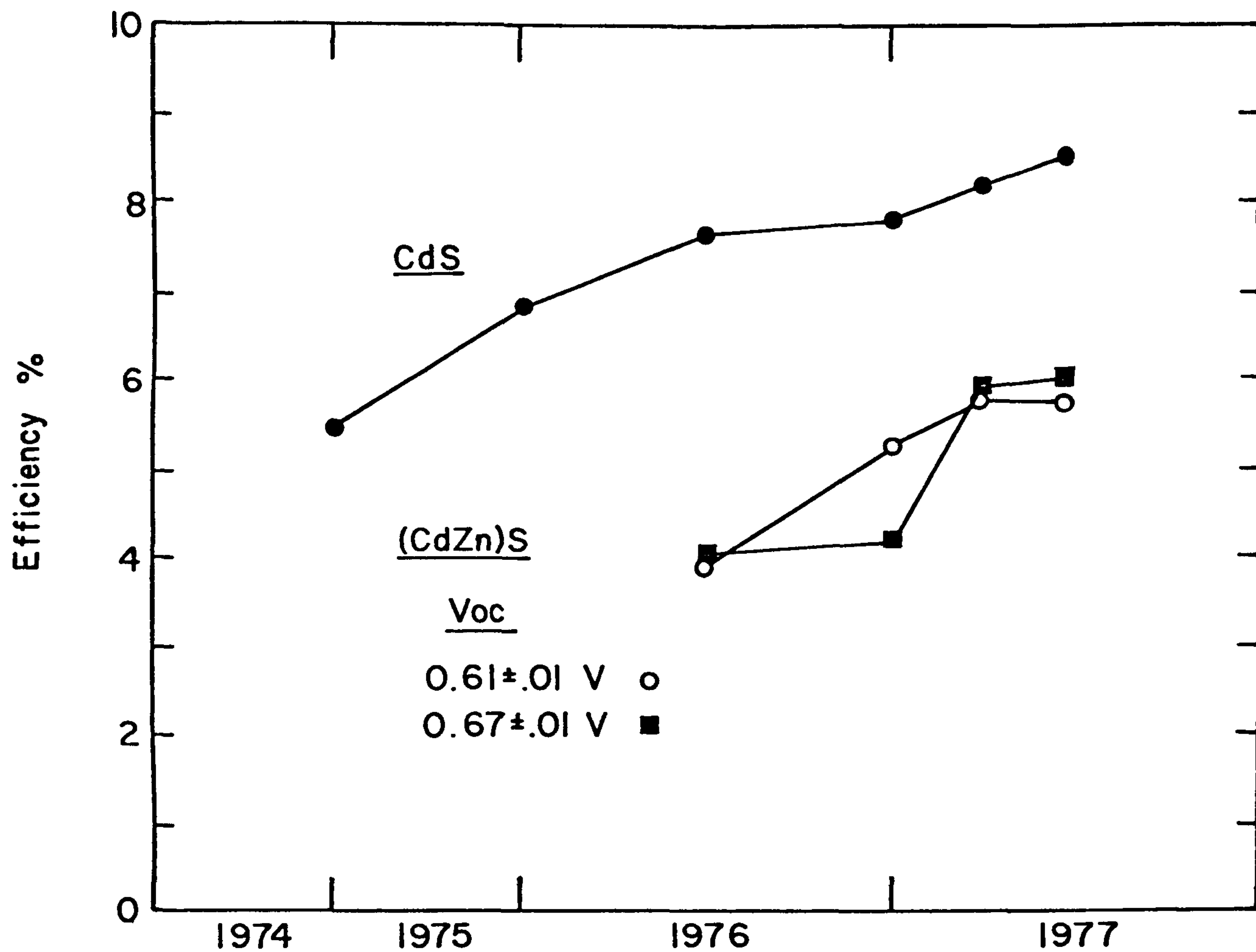

Figure 2. Chronological development of power conversion efficiency for both CdS/Cu_2S and $(CdZn)S/Cu_2S$ cells.

4. Introduction

The program goal is the production of a thin film polycrystalline cell with a 10% power conversion efficiency. Two related heterojunctions are being developed, the CdS/Cu_2S and $(CdZn)S/Cu_2S$. The yield of high efficiency CdS/Cu_2S cells is good with only one cell out of 47 having zero output. Over half of the cells would exceed 7.5% efficiency in sunlight. Work has continued to improve the production control and to optimize the properties of the (CdZn)S films. The maximum efficiency achieved with the $(CdZn)S/Cu_2S$ cell has reached 6.29%.

This program was based on the previous NSF/RANN program summarized in reference 1. Three quarterly progress reports, references 2, 3 and 4 should be examined for detailed experimental results. The primary theoretical analysis of this type of solar cell is given in reference 5 and attached as Appendix B. Key progress is summarized in reference 6, Appendix C for the CdS/Cu_2S cell and reference 7, Appendix D for the $(CdZn)/Cu_2S$ cell.

4.1 Objectives

The long term objective of the present program is a low cost thin film polycrystalline cell for terrestrial power generation. The immediate objective is to increase the power conversion efficiency of laboratory cells to more than 10%. Materials and electro-optical analyses are conducted in order to quantify the structure and the properties necessary to achieve such efficiency. As higher efficiencies are reached, increasingly sophisticated and precise characterization techniques become necessary and are being developed as part of this program.

4.2 Approach and Key Methods

The basic cell formation procedure continues to be the vapor deposition of a CdS or (CdZn)S layer. The p-type Cu_2S layer is being produced by either solution or solid state reaction with cuprous chloride. The key to the continued improvement in thin film performance is the close coupling of analytical techniques and modeling with the cell production. Quantitative loss analysis for the particular cell design being produced directs the selection of improvement modifications and establishes when specific design limits have been reached.

5.1 Development of CdS/Cu_2S Cells

During this quarter, the experiments on etched (textured) cells with evaporated grids and an SiO anti-reflection coating have been continued. Good yield was achieved and as reported previously, a maximum efficiency of 8.5% recorded in actual sunlight testing.

Cell Production

A total of 47 cells were made with grids of either 60 or 80 lines per inch. All cells were given at least one heat treatment in H_2/Ar although only a selected number of cells were given complete optimization treatments. Nevertheless, the average efficiency of all the cells including the one shorted cell with zero output, was 6.4% in the W-I simulator; on the basis of the eight cells tested in sunlight, the ratio between sunlight and W-I testing is 1.14 and hence the deduced average sunlight efficiency is 7.2%. A histogram of the computed sunlight efficiencies is shown in Figure 3. Over half the cells would exceed 7.5% efficiency in sunlight.

5.2 Development of (CdZn)S/Cu_2S Cells

Development of a reproducible deposition technique for low resistivity homogeneous (CdZn)S films has continued. Some capacitance measurements are reported showing the influence of the mixed sulfide on the rate of copper compensation.

Table 1

Testing under W-I Simulation of 47 Cells with Textured Surfaces, Evaporated Grids and an SiO Anti-Reflection Coating.

Cell #	Cu_2S (μm)	Grid (ℓ.p.i.)	J_{sc} (mA/cm^2)	V_{oc} (v)	FF (%)	Eff. W-I (%)
456 A2-2	0.18	60	17.86	0.478	53.0	4.52
A2-3	"	"	21.69	0.481	65.3	6.81
A2-4	"	"	19.17	0.485	62.9	5.85
442 B1-1	0.36	"	24.02	0.491	62.7	7.40
449 B1-2	"	"	18.44	0.503	72.6	6.73
B1-3	"	"	19.69	0.499	68.8	6.76
455 B1-3	"	"	20.32	0.502	67.7	6.91
456 B2-2	"	"	19.55	0.501	69.5	6.81
B2-3	"	"	19.39	0.504	69.5	6.79
B2-4	"	"	19.68	0.507	70.0	6.98
458 B2-1	"	"	17.17	0.503	65.0	5.61
B2-2	"	"	18.70	0.502	65.8	6.19
B2-3	"	"	17.63	0.505	66.4	5.91
B2-4	"	"	17.65	0.505	65.0	5.79
460 B2-1	"	"	19.51	0.509	64.7	6.41
B2-2	"	"	20.51	0.504	62.5	6.46
B2-3	"	"	22.22	0.496	62.8	6.92
B2-4	"	"	21.51	0.502	64.3	6.94
458 A2-1	0.48	"	19.44	0.503	65.9	6.44
A2-2	"	"	21.03	0.515	64.0	6.93
A2-3	"	"	18.99	0.501	66.1	6.29
A2-4	"	"	20.80	0.506	64.9	6.83
456 A1-2	0.18	80	18.55	0.481	61.0	5.44
A1-3	"	"	18.42	0.467	63.2	5.44
460 A1-1	0.24	"	19.64	0.505	69.4	6.44
A1-2	"	"	20.83	0.508	63.5	6.72
A1-3	"	"	21.11	0.508	64.5	6.92
A1-4	"	"	20.50	0.504	64.8	6.69
455 B2-1	0.36	"	20.00	0.508	7.01	7.12
B2-2	"	"	19.06	0.507	69.2	6.69
B2-3	"	"	18.94	0.503	70.5	6.72
B2-4	"	"	19.83	0.506	69.1	6.94
456 B1-2	"	"	19.29	0.506	69.2	6.75
B1-3	"	"	16.29	0.499	69.3	5.63
B1-4	"	"	17.73	0.504	68.2	6.09
458 B1-1	"	"	18.30	0.498	66.0	6.00
B1-2	"	"	21.28	0.493	62.1	6.52
B1-3	"	"	0	0	0	0
B1-4	"	"	17.20	0.503	66.8	5.79
460 B1-1	"	"	20.69	0.506	67.5	7.07
B1-2	"	"	19.85	0.503	67.6	6.75
B1-3	"	"	20.87	0.508	67.1	7.11
B1-4	"	"	22.19	0.492	63.8	6.97
458 A1-1	0.48	"	19.47	0.504	67.1	6.58
A1-2	"	"	19.50	0.509	68.4	6.78
A1-3	"	"	18.90	0.496	66.9	6.28
A1-4	"	"	22.54	0.511	65.4	7.54

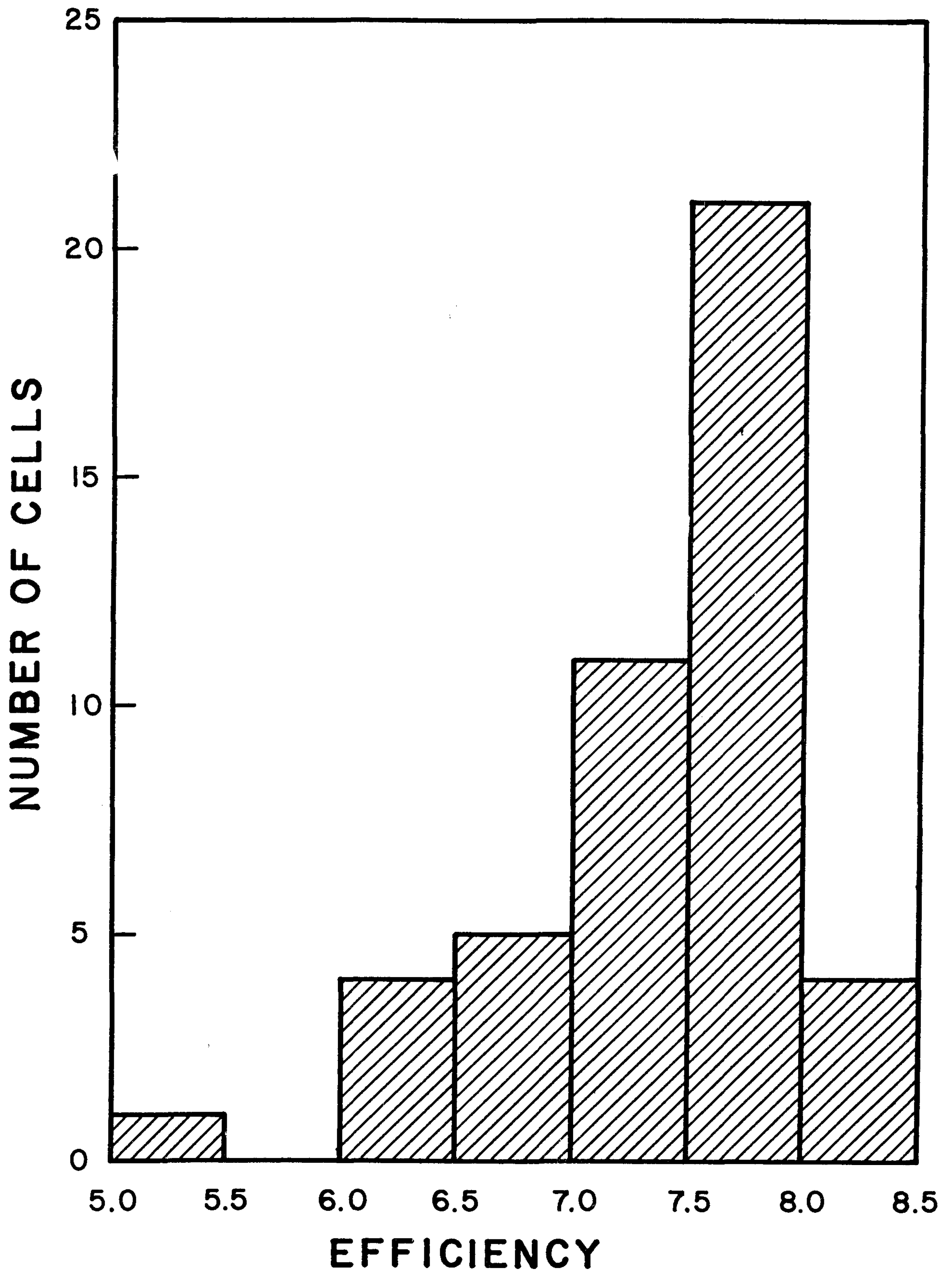

Figure 3. Distribution of efficiencies for 47 cells. Natural insolation values deduced from simulator tests.

Growth of (CdZn)S Films

During the last reporting period, the concentric evaporation source was used to produce mixed sulfide films with resistivities of $\gtrsim 50\ \Omega$ cm at zinc contents of $\sim$ 20%. Further optimization of deposition conditions has resulted in films of 1 Ω cm resistivity with zinc contents up to $\sim$ 10%. At higher zinc levels, the deposition rate necessary to achieve low resistivity is too high for good control ($\sim$ 7 μm/minute) and accordingly the source orifice size is being reduced.

(CdZn)S/Cu_2S Cells

Some measurements of cell capacitance as a function of zinc content were reported last quarter.[4] Further experiments have been conducted and the effects of heat treatment on (CdZn)S cells compared to that on CdS cells, Table 2. CdS #445 has a specific resistivity of 2.4 Ω cm and (CdZn)S #430 contains 16% zinc and is 100 Ω cm material.

Table 2

Influence of 16 Hour Heat Treatments on the Capacitance of CdS/Cu_2S Cells (445) and (CdZn)S Cells (430). The Values Given are the Mean of Two Cells.

Cell #	Temp (°C)	C/A (nF/cm^2)
445 D	150	25
445 C	225	0.66
445 F	300	0.67
430 D	150	26
430 C	225	2.4
430 F	300	0.58

All cells are exposed to a thermal treatment of 190°C for 30 minutes during the gridding stage before the above treatments. It is seen that the mixed sulfide is compensating more slowly than the CdS but seems to reach the same order of limiting capacity (see ref 4, p. 66).

5.3 Electro-Optical and Theoretical Analysis

Refined estimates have been made of the influence of CdS resistivity on achievable open circuit voltage and compared to actual values. The true junction area also influences V_{oc} and a number of techniques have been used to determine the ratio of cell area to total junction area.

The power conversion efficiency is adversely influenced by low shunt resistances (R_{SH}) and high series resistances (R_s). Conventional use of dV/dI at V = 0 and V = V_{oc} can give spurious values of the resistivity components particularly in the presence of voltage dependent current collection. Alternative ways of measuring R_{SH} and R_s are discussed and the influence of these terms on fill factor is described.

Finally, some relationships between Cu_2S stoichiometry and optical properties and cell performance are developed.

5.3.1. Variation of V_{oc} with CdS Resistivity

In previous reports[2,3] expressions for V_{oc} as a function of CdS resistivity or the ratio $r = N_{DCdS}/N_{ACu_2S}$ have been derived. In reference 3 the expression given is

$$V_{oc} = \frac{(E_g - \Delta X - \delta_1)}{q} - \frac{kT}{q} \ln \frac{qN_{c2} S_I (A_j/A_\perp)}{j_L (V_{oc})}$$

$$- \frac{N_D}{N_A} \left(\frac{kT}{q} \ln \frac{qN_{c2} S_I (A_j/A_\perp)}{j_L (V_{oc})} - \delta_2\right)$$

where E_g is the Cu_2S band gap $\simeq$ 1.2 eV, ΔX the difference in electron affinities between Cu_2S and CdS $\simeq$ 0.2 eV, N_{c2} the effective density of stages at CdS band edge $\simeq 2 \times 10^{18}/cm^3$, S_I the interface recombination velocity $\simeq 10^6$ cm/sec, $A_j/A_\perp$ the ratio of junction area to planar area, $j_L (V_{oc})$ the light generated current at V_{oc}, N_D the donor density in CdS, N_A the acceptor density in Cu_2S, δ_1 position of the Fermi level in bulk Cu_2S relative to the valence band and δ_2 that in CdS relative to the CdS conduction band. For non-degenerate materials $\delta_1 = kT \ln N_{v1}/N_A$, $\delta_2 = kT \ln N_{c2}/N_D$. With $N_{v1} \simeq 10^{19}/cm^3$ and $N_A = 10^{18} - 10^{19}/cm^3$ the Cu_2S is in the degenerate range and tables of Fermi integrals must be used to obtain δ_1. At 300°C, δ_1 ($N_A = 10^{18}/cm^3$) = 0.06 eV, δ_1 ($N_A = 5 \times 10^{18}/cm^3$) = 0.13 eV, δ_1 ($N_A = 10^{19}/cm^3$) = -.01 eV. Using $N_D = (q\mu_{CdS} \rho_{CdS})^{-1}$, with μ_{CdS} = 20-100 cm^2/vs we can calculate the expected variation of V_{oc} with ρCdS and compare the results with experimental results.

Table 3 gives V_{oc}, j_{sc}, $\bar{d}Cu_2S$ and ρCdS for a number of cells prepared using the dry process to form the Cu_2S layer. These cells are expected to have higher V_{oc}'s than wet process cells due to smaller $A_j/A_\perp$ value, since formation of Cu_2S in grain boundaries doesn't occur in dry process. In some instances the V_{oc} values drifted down as a function of time and a range of values is listed. The time drift may be due to the build up of positive charge in the space charge region of the CdS in the

light. The measured j_{sc} values were all within 2 mA/cm^2 of 13 mA/cm^2 and the V_{oc}'s were normalized to this value.

Table 3

Cell #	ρ_{CdS}	V_{oc}	j_{sc} $(\frac{mA}{cm^2})$	$\bar{d}$ (A°)
366	1.18	.522 - .533	13	1400
358C	1.25	.508 .518	13	1905
360	1.47	.515	13	2900
375	2.1	.540	13	928
444	2.9	.52 - .546	13	334
461 A-1	3.9	.52 - .55	13	1014
461 C-1	3.9	.537	13	1990
462 A-1	6.5	.52 - .55	13	1014
465 A-1	13.5	.541 .536	13	1993
465 A-2	13.5	.533	13	1993

The data shows a variation in V_{oc} with ρ which is consistent with the predictions of the model. However, the range of ρ values particularly at the low end is not wide enough to allow quantitative comparisons to be meaningful. The uncertainty of $A_j/A_{\perp}$, μCdS, S_I and the differences in N_A from sample to sample also introduce errors too large to allow firm conclusions to be reached.

5.3.2. Estimates of Surface and Junction Area

The surface of the evaporated CdS layer is not flat and consequently the Cu_2S-CdS junction area is larger than the planar area of the cell. In the usual cell fabrication, the CdS is etched before formation of the Cu_2S layer. This further increases the surface and junction area. Since the surface area enters into the determination of the open circuit voltage of the cell, its value is of interest.

We have used two methods to estimate the surface area of the cells. One involves the chemically determined thickness, $\bar{d}$, of the Cu_2S layer formed by the wet process, the other the capacitance of dry processed cells.

In reference (3) we analyzed data on $\bar{d}$ versus dip time, to obtain the rate limiting diffusion coefficient in the wet process cells. The equation used was

$$\bar{d}\ (t) = T\ C_1\ t^{\frac{1}{2}} + \frac{c_1 c_2}{r}\ t \tag{2-1}$$

where T was the ratio of the true surface area to the geometrical area of the cell. The value of T is expected to differ for etched and unetched material. Hence, for otherwise identical material we can write $\Delta\bar{d} = \bar{d}_{etch} - d_{unetched} = (T_E - T_u)\ c_1\ t^{\frac{1}{2}}$ and obtain the difference in surface area between etched and unetched material from a plot of $\Delta\bar{d}$ versus $t^{\frac{1}{2}}$ and the previously determined value of c_1. The data presented in ref (3) was for substrate 124 unetched and 126,3 sec etch. The analysis of this data gives $c_1 \simeq 245$ Å$/s^{\frac{1}{2}}$, $d\Delta\bar{d}/dt^{\frac{1}{2}} = 160$ Å$/s^{\frac{1}{2}}$ and

$$T_E = T_u + .65 \tag{2-2}$$

This indicates that the 3 second etch increases the surface area by less than a factor of two since the minimum value of T_u is 1.

An estimate of the value of T_u can be obtained from capacitance values of etched and unetched material prepared by the dry technique. The capacitance per unit planar area is given by

$$\frac{C}{A_{\perp}} = T\ \frac{\varepsilon\varepsilon_0}{w} = \frac{\varepsilon\varepsilon_0}{w_{calc}} \tag{2-3}$$

where w_{calc} is the value of w the space charge width calculated from the measured capacitance when T is assumed to be unity. In table 4 we list the data for cells 461C1 unetched, and 461D1 4 sec etch. From Eq (2-3) we have under the assumption that w is the same for etched and unetched material, the relation

$$\frac{T_E}{T_u} = \frac{(W_{calc})_u}{(W_{calc})_E} \qquad (2\text{-}4)$$

The data indicates $T_E/T_u \simeq 1.35$. If we assume that result Eq (2-2) holds for these cells (note 3 sec etch versus 4 sec etch) then we have

Table 4

Cell	w_{calc} before heat treatment	w_{calc} after HT	
461 C1	0.73 μm	1.33 μm	unetched
461 D1	0.56	0.96	etched
$\frac{(w_{calc})}{(w_{calc})_E}$	1.30	1.39	

$$T_u = 1.86 \; ; \; T_E = 2.51 \qquad (2\text{-}5)$$

These results are only estimates since the $\bar{d}$ analysis has large uncertainties, and the capacitance data will only reveal structure which is large compared to w. Since w is on the order of 1 μm, structure on a finer scale will not be detected by the capacitance measurements. The junction area, however, will follow variations which are on the scale of d_1 the midgrain thickness which is $d_1 = c_1 t^{1/2}$, for typical cells t ranges from 6s to 12 sec giving d_1 values of between 600 Å and 850 Å. Hence, on the scale of interest the capacitance technique may not be giving as accurate

a reading as desired. However, Eq (2-2) sets an upper limit of T_E/T_u of 1.65 (when $T_u = 1$), and the results in Eqs (2-5) are reasonable.

An analysis of SEM pictures of unetched and etched CdS Figs. 4a and 1b respectively, give estimates which are in accord with those above. Fig. 4b shows the unetched material to consist of roughly hemispherical mounds with radii of 5-10 μm. For hemispherical caps $T_u = 2$. The etched material shows triangular pyramids with roughly equal peak heights and base widths and 90° peak angles. Such pyramids would give T_E on a planar surface of $(3)^{1/2}$. Cones would give T_E on a planar surface of $\sqrt{2}$. Since the pyramids are formed in the hemispherical mounds, T_E/T_u values less than the theoretical ones are expected. The size of the features of the etched material range from ∿ .1 μm to 2 μm. Hence our methods based on $\bar{d}$ and capacitance appear to be sensitive enough to give reasonable estimates of T_E and T_u.

5.3.3. Series Resistance Determination from I-V Curves

In the diode equation for the cell the cell's series resistance R_s enters as an important parameter. We have previously treated[2,3] the dependence of the fill factor on the series resistance, and indicated that the value of R_s can be determined from plots of fill factor versus intensity (short circuit current). A common procedure for evaluating R_s from the I-V curve in the light is to use the slope at V_{oc} i.e.

$$\left(\frac{dV}{dI}\right)_{V_{oc}} = R_s + \frac{kT}{qI_L} \tag{3-1}$$

where $I_L = I_{sc}$ is usually assumed. While Eq (3-1) is valid for silicon cells, and some CdS/Cu_2S cells yield R_s values from Eq (3-1) that are in

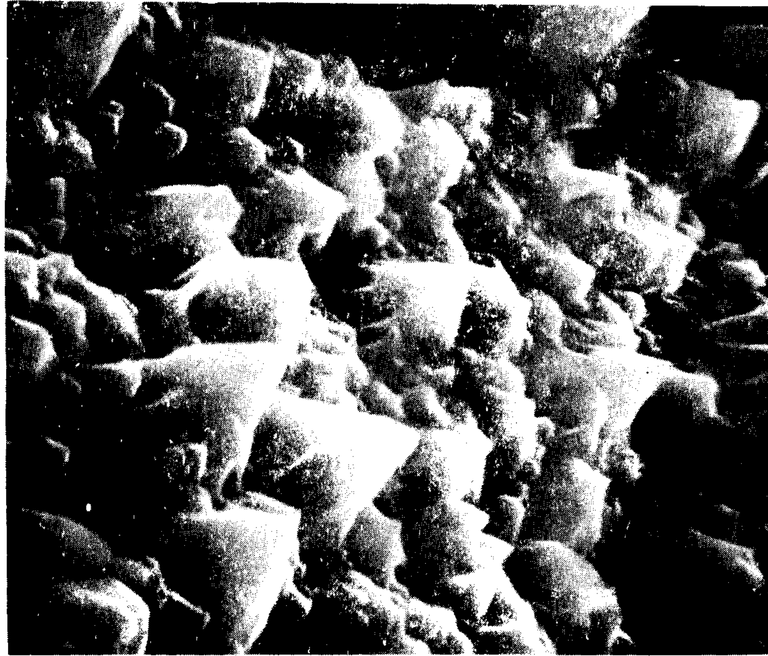

(a)

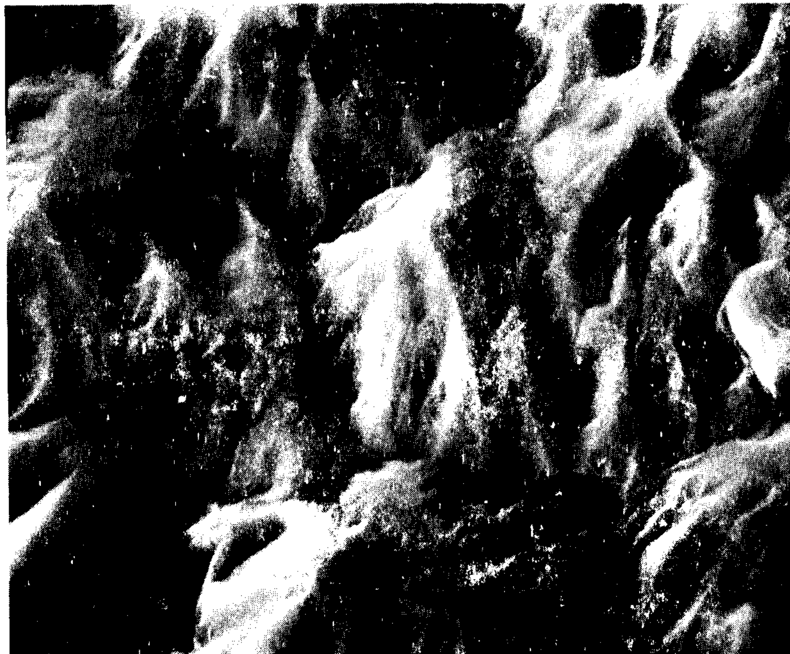

(b)

Figure 4. Surface structure of textured (etched) and as deposited CdS

excellent agreement with those obtained from the fill factor versus intensity plots, it is not valid when I_L has a strong dependence on voltage.

This is particularly evident for CdS/Cu_2S cells illuminated with long wavelength light. Under those circumstances Eq (3-1) should be replaced by

$$\left(\frac{dV}{dI}\right)_{V_{oc}} = \left(R_s + \frac{kT}{qI_L(V_{oc})}\right) / \left(1 + \frac{kT}{qI_L(V_{oc})} \; / \; \frac{dI_L(v)}{dV}\right)_{(V_{oc})} \qquad (3\text{-}2)$$

If we use current densities instead of currents, we can insert typical values into (3-2), with A the cell area we have

$$\left(\frac{dV}{dj}\right)_{V_{oc}} = \left(R_s A + \frac{kT}{qj_L(V_{oc})}\right) / \left(1 + \frac{kT}{qj_L}(V_{oc}) \left|\frac{dj_L(v)}{dV}\right|_{V_{oc}}\right) \qquad (3\text{-}3)$$

For $j_L(0) \simeq .02$ Amp/cm^2, $kT/qj_L = 1.30\ \Omega$ cm^2 at 300°K. If j_L falls to half its V = 0 value at V_{oc} (an extreme case) and we assume a linear dependence then the numerator of (3-3) increases by ∿ 50% while the denominator increases by ∿ 2%. Hence, the main effect of the voltage dependence of j_L appears in the numerator, and if the I-V curve is analyzed using Eq (3-1) instead of (3-3) an erroneously large R_s would be obtained.

The data in Table 5 illustrates the marked difference in the apparent series resistance when Eq. (3-1) is used. Using the variation of fill factor with intensity (Fresnel and AM1 readings) gives $R_s A \simeq 0.92$ ohm-cm^2 for this cell. The variation in fill factor illustrated in Table 5 results from changes in the light induced junction field and is treated more fully below.

Table 5

Cell 455 B2-2 Under Various Illumination

Illumination	j_L (mA/cm^2)	FF	R_sA (Eq (3-1))	$R_sA = .92\ \Omega\ cm^2$ $\frac{j_L(V_{oc})}{j_L}$	$.98\ \Omega\ cm^2$ $\frac{j_L(V_{oc})}{j_L}$
∿ 6.3 x AM1	118	.538	1.0	.732	.916
$\lambda < 0.59$ μm	18.6	.710	1.16	.853	.886
AM1	18.6	.679	1.8	.613	.629
$\lambda > 0.54$ μm	∿ 19.0	.565	3.6	.455	.476
$\lambda > 0.58$ μm	∿ 19.0	.514	3.4	.355	.357

Neglecting the correction term in the denominator of Eq (3-3) we have

$$R_sA = \frac{dV}{dj})_{V_{oc}} - \frac{kT}{qj_L}(V_{oc})$$

$$= [\frac{dV}{dj})_{V_{oc}} - \frac{kT}{qj}] - \frac{kT}{qj_L}\left(\frac{j_L}{j_L(V_{oc})} - 1\right)$$

$$= R_s{'}A - \frac{kT}{qj_L}\left(\frac{j_L}{j_L(V_{oc})} - 1\right) \quad (3\text{-}4)$$

Where $R_s{'}A$ is the value one would have calculated using Eq (3-1). Having determined R_sA from fill factor versus intensity, and also $R_s{'}A$, $j_L(V_{oc})$ can be obtained from Eq (3-4) i.e.

$$\frac{j_L(V_{oc})}{j_L} = \frac{kT}{qj_L\left(R_s{'}A - R_sA + \frac{kT}{qj_L}\right)} \quad (3\text{-}5)$$

The results are sensitive to the R_sA value assumed. Table 5 gives $j_L(V_{0\varepsilon})/j_L$ values for R_sA values 0.92 ohm cm^2 and .98 Ω cm^2. The latter value gives results closer to those expected but the AM1 simulation value still seems lower than expected. Studies of additional cells will yield characteristic values for the various illumination.

5.3.4. Light Dependent Apparent Shunt Resistance

The full expression for the current voltage relation of the cell can be written as

$$I = I_0\left[\exp\frac{q(V - IR_s)}{AkT} - 1\right] - I_L(V) + \frac{V - IR_s}{R_{sh}} \quad (4\text{-}1)$$

where I_0 is the dark saturation current, A the diode ideality factor and R_{sh} the shunt resistance. A common practice for evaluating R_{sh} is to use the slope of the curve in reverse bias, particularly at V = 0. Using Eq (4-1) we have

$$\left.\frac{dV}{dI}\right)_{V=0} = \frac{R_{sh} + R_s \left[1 + R_{sh} \frac{q}{AkT} I \exp\left(\frac{-qIR_s}{AkT}\right)\right]}{1 + R_{sh} I \frac{q}{AkT} \exp\left(\frac{-qIR_s}{AkT}\right) - R_{sh} \left.\frac{dI_L(V)}{dV}\right)_{V=0}} \qquad (4\text{-}2)$$

For all cells of interest $R_{sh} >> R_s$, and $AkT/qI_0 >> R_{sh}$. Hence, Eq (4-2) reduces to

$$\left.\frac{dV}{dI}\right)_{V=0} = \frac{R_{sh}}{1 - R_{sh} \left.\frac{dI_L(V)}{dV}\right)_{V=0}} \qquad (4\text{-}3)$$

For the dark (I_L = 0) the slope at V = 0 gives R_{sh}. In the light, however, the dI_L (V)/dV term tends to reduce the value of the slope. If we assume that $I_L = I'_L f(V)$ where I'_L is voltage independent, and linearly dependent on light intensity, while f(V) is voltage dependent and independent of intensity (it may depend on wavelength of light), then we have

$$R'_{sh} = \left.\frac{dV}{dI}\right)_{V=0} = \frac{R_{sh}}{1 - R_{sh} I'_L \left.\frac{df(V)}{dV}\right)_{V=0}} \qquad (4\text{-}4)$$

$$\frac{R_{sh}}{R'_{sh}} = 1 - R_{sh} I'_L \left.\frac{df(V)}{dv}\right)_{V=0} \qquad (4\text{-}5)$$

Experimental data from cells tested under various intensities can be used to test the validity of Eq (4-5). In Table 6 data for two cells is given.

In Fig. 5 we have plotted this data using j_{sc} to approximate I'_L. The linearity of the result agrees well with Eq (4-5) and the slope of the

Table 6

Apparent Shunt Resistance as a Function of Illumination

Illumination	R'_{sh} ohm	j_{sc} (mA/cm^2)	$-\frac{df(V)}{dV})_0$
Cell 457 A1-4			.0296
dark	1760	-	
25% AM1	1040	3.8	
55% AM1	892	7.96	
75% AM1	847	11.7	
100% AM1	866	15.1	
Cell 457 A2-3			0.0357
dark	6700	-	
25% AM1	2500	4.0	
55% AM1	1840	8.28	
75% AM1	1490	12.1	
100% AM1	1220	16.0	

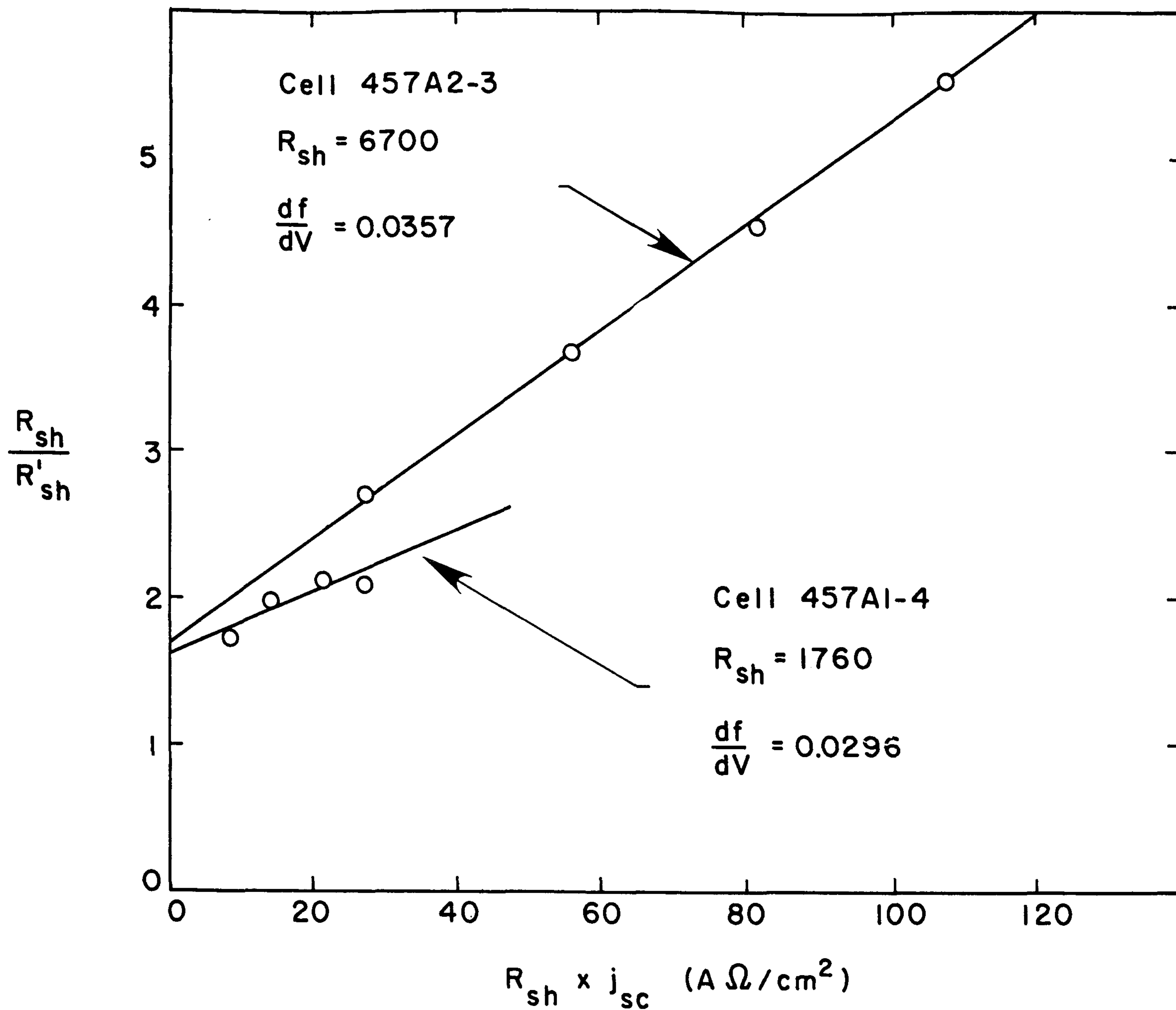

Figure 5. Dependence of light sensitive shunt resistance on short circuit current.

curve has been used to obtain the $df/dV/_{V=0}$ values listed in Table 4. However, the curves do not have the y intercept of unity as predicted by Eq (4-5). This is probably due to an intensity dependence of f(V) at low intensities, which we have omitted in Eq (4-5).

We can relate the variation of I_L with voltage to the basic junction properties of the cell. In a previous report[2] the expression for j_L (V) given was

$$j_L = j_{LO} \frac{\mu_2 F_2 (V)}{S_I + \mu_2 F_2 (V)} \tag{4-6}$$

where j_{LO} is proportional to light intensity and independent of voltage (except in the special circumstance that the Cu_2S and CdS doping levels are nearly equal), while $F_2(V)$ is the voltage dependent junction field, μ_2 the CdS mobility and S_I the effective interface recombination velocity are assumed to be independent of both light intensity and voltage. The expression for F (V) is

$$F (V) = F_L + [2(V_D^* - V) qN_D^*/\varepsilon\varepsilon_0]^{1/2} \tag{4-7}$$

with F_L the field resulting from the ionization of deep compensating centers by light and the uncovering of deep donor levels near the junction, V_D^* is that part of the diffusion voltage supported by the remaining space charge, and $N_D^* = (N_D - N_A)$ is the net donor concentration in the compensated region. Using

$$f(V) = \frac{\mu_2 F_2 (V)}{S_I + \mu_2 F_2 (V)} \tag{4-8}$$

we have

$$\frac{df(V)}{dV} = \frac{f(V)(1 - f(V))}{F_2 (V)} \quad \frac{d F_2 (V)}{dV}$$

$$= \frac{S_I \mu_2}{(S_I + \mu_2 F_2 (V))^2} \quad \frac{d F_2 (V)}{dV} \qquad (4\text{-}9)$$

$$= \frac{S_I \mu_2}{(S_I + \mu_2 F_2 (V))} \quad \left(\frac{2 V_D^* qN_D^*}{\varepsilon\varepsilon_0}\right)^{\frac{1}{2}} \frac{1}{2V_D^* (1 - \frac{V}{V_D^*})^{\frac{1}{2}}}$$

For V = 0 we have

$$\left.\frac{df(V)}{dV}\right)_{V=0} = \frac{S_I \mu_2}{(S_I + \mu_2 F_2 (V))^2} \left(\frac{2 V_D^* q N_D^*}{\varepsilon\varepsilon_0}\right)^{\frac{1}{2}} \frac{1}{2V_D^*}$$

If we define $F (V_D^*) = (2 V_D^* q N_D^*/\varepsilon\varepsilon_0)^{\frac{1}{2}}$ we can write

$$\left.\frac{df(V)}{dV}\right)_0 = \frac{f(o)(1 - f(o))}{2V_D^*} \quad \frac{F(V_D^*)}{F_2 (o)}$$

For typical values $f(o) \simeq .9 - .95$, $V_D^* \sim .25$ V, $F(V_D^*) \simeq 10^3$ v/cm, $S_I \simeq 10^5 \sim 10^6$ cm/sec, $\mu_2 \simeq 50\text{-}100$ cm/vs indicate $F_2 (o) = 10^4 - 10^5$ V/cm and $df/dV)_0$ values of 10^{-3} to .02, with the higher values occurring for lower $F_2(o)$ and S_I values and higher μ_2 values. Lower f(o) values will also yield high df/dV values.

The above analysis neglects the uncovering of deep levels in the CdS near the junction. These levels are responsible for the form of the $1/c^2$ versus voltage plots, which typically are flat for voltages less than $\sim$ 0.4 V. Hence, the expression for F_2 (V) given in Eq (4-7) should be modified to include the effects of deep levels. The inclusion of these effects should yield closer agreement with experimental results.

5.3.5. Fill Factor Expression

In previous treatments the various causes of fill factor loss (1) series resistance, (2) field dependent j_L, and (3) shunt resistance, have been treated separately. An expression for the fill factor which combines these separate terms can be written in analytic form when each of the loss terms accounts for no more than $\sim$ .1 loss in fill factor. This expression is

$$FF = FF_0 \left(\frac{qV_{oc}}{kT}\right) - C \left(\frac{qV_{oc}}{kT}\right) \frac{j_{sc} R_s A}{V_{oc}}$$

$$- \frac{V_{mp}}{V_{oc}} S_I \frac{(1 - F_2 (V_{mp})/F_2(o)}{(S_I + \mu_2 F_2 (V_{mp}))} - \frac{V_{mp}}{V_{oc}} \frac{V_{mp}}{j_{sc} A R_{sh}}$$

where the first term is the theoretical lossless fill factor as a function of (V_{oc}/kT), the second the linearized series resistance loss term with A the cell area and C $\left(\frac{qV_{oc}}{kT}\right)$ on the order of 0.9 and weakly dependent on (qV_{oc}/kT), the third term results from the voltage dependence of j_L, and the fourth from the shunt resistance of the cell, V_{mp} is the voltage at the maximum power point.

5.3.6. Relation of Cu_2S Resistivity to Optical and Infrared Absorption Coefficients, and to the Short Circuit Current of CdS/Cu_2S Cells

Experimental evidence exists which shows a direct relation between the resistivity (obtained as sheet resistance) of the Cu_2S layer the optical ($\lambda <$ 1 μm) absorption coefficient, the infrared ($\lambda >$ 1 μm) absorption coefficient, and the short circuit current of the CdS/Cu S solar cell. These relations can be summarized as follows

(1) $\alpha_{optical}$ increases with increasing ρ

(2) $\alpha_{infrared}$ decreases with increasing ρ

(3) $j_L \sim \rho^{1/2}$

Difficulties in obtaining theoretical expressions which exhibit the above relations involve (a) the hole concentration in $Cu_{2-x}S$ depends on x and so does the mobility;[8] (b) theoretical expressions for the optical absorption coefficient of degenerate materials differ in their dependence on scatterer density,[9,10] (c) the classical expression for the infrared (free carrier) absorption is not valid, and the quantum mechanical expressions differ depending upon the dominant scattering mechanism[10] (d) since j_L depends upon the Cu_2S absorption coefficient and the diffusion length and both are changing, the dominant mechanism leading to relation (3) is not clear.

Previous attempts[11-13] to explain relation (3) have suggested that changes in the recombination lifetime with carrier concentration were responsible i.e. for constant Cu_2S thickness $j_L \sim L_n$ and

$$L_n = \left(\frac{kT}{q} \mu_n \tau_n\right)^{1/2} \tag{6-1}$$

If $\tau_n \simeq \frac{c}{p}$ and with $\rho = \frac{1}{q \mu_p p}$ one has

$$L_n = \left(\frac{kT}{q} \mu_n q \mu_p c \rho\right)^{1/2} = \left(\frac{kT}{q} \mu_n \mu_p q\right)^{1/2} \rho^{1/2}$$

Hence, if μ_n and μ_p were independent of p, relation (3) would be obtained. Various mechanisms which would give $\tau \sim 1/p$ have been suggested previously,[12,13] they include radiative recombination, trap densities proportional to hole concentration, and auger recombination through traps.

The possibility that the mobility changes with hole concentration through the dominance of impurity scattering was also suggested. In view of the strong variation in mobility with stoichiometry recently reported[8] in the stoichiometry range of interest, this possibility was reinvestigated. Based on data[9] from heavily doped Ge, one can expect $\mu \sim N^{-\frac{1}{2}}$. If we set N = p we have

$$p \sim \frac{1}{p^{\frac{1}{2}}} \text{ and } L_n \sim p^{-\frac{1}{4}} \text{ if } \tau_n$$

is independent of p. This would give relation (3). Theoretical expressions[10] for μ as a function p are approximate and give no simple expression valid through the range of p of interest.

6. References

1. Final Report, NSF/RANN/AER72-03478 A04 FR/76, March 1977.

2. E(49-18)-2538 PR76/1

3. E(49-18)-2538 PR76/2

4. E(49-18)-2538 PR77/1

5. A. Rothwarf and A. M. Barnett, IEEE Transactions on Electron Devices, Vol. ED-24, No. 4, April 1977.

6. A. M. Barnett, J, D. Meakin, A. Rothwarf, Progress in the Development of High Efficiency Thin Film Cadmium Sulfide Solar Cells, Luxembourg, September 1977.

7. L. C. Burton, B. Baron, T. L. Hench, J. D. Meakin, Formation and Characterization of (CdZn)S Films and (CdZn)S/Cu_2S Heterojunctions, 19th Annual Electronic Materials Conference, Cornell University, 1977.

8. S. Z. Idrichan and G. P. Sorokin, Inorganic Materials 11, 1449 (1975).

9. J. I. Pankove, Progress in Semiconductors 9, 48 (1965), Optical Processes in Semiconductors, Prentice Hall, Englewood Cliffs, N. J., 1971, p. 40, 76.

10. V. I. Fistul', Heavily Doped Semiconductors, Plenum Press, N. Y., 1969, pp. 92-95, 208-211.

11. H. Hadley and W. Nelson, NSF/RANN/SE/GI 347872/TR73/13, September 1973.

12. Quarterly Progress Report, NSF/RANN/SE/GI-34872/PR74/1, April 1974, p. 32.

13. Quarterly Progress Report, NSF/RANN/SE/GI-34872/PR74/2, August 1974, p. 66.

Appendix A

LIST OF RESEARCH CONTRIBUTORS

Dr. John D. Meakin, Associate Director, Principal Investigator

Dr. Allen M. Barnett, Director

Dr. Bill N. Baron, Associate Scientist

Dr. Charles E. Birchenall, Distinguished Professor of Metallurgy

Dr. Larry C. Burton, Scientist

Dr. Walter E. Devaney, Research Associate

Mr. Thomas L. Hench, Research Assistant

Ms. Leslie M. Kilgren, Research Associate

Mr. Steven Lorenz, Electronics Engineer

Mr. James V. Masi, Program Development Manager, Photovoltaics

Mr. George Miller, Senior Laboratory Technician

Dr. Roy L. McCullough, Professor of Chemical Engineering

Mr. Patrick Mulvihill, Graduate Student

Dr. Larry D. Partain, Assistant Professor of Electrical Engineering

Mr. James E. Phillips, Research Associate

Dr. Allen Rothwarf, Senior Scientist

Dr. Joseph Sansregret, Research Associate

Mr. Stephen Shea, Graduate Student

Dr. George Storti, Research Associate

Mr. David Brindle, Instrument Technician

Mr. David Cowgill, Senior Design Machinist

Ms. Gwendolyn A. Howk, Senior Research Technician

Mr. Thomas Lovett, Undergraduate

Ms. Maryanne Powers, Senior Research Technician

Mr. Robert Wieland, Research Technician

Mr. Walter Willing, Undergraduate

Mr. David Potts, Graduate Student

Ms. Sandra Lynn Matthews, Senior Secretary

Appendix B

IEEE TRANSACTIONS ON ELECTRON DEVICES, VOL. ED-24, NO. 4, APRIL 1977 381

Design Analysis of the Thin-Film CdS–Cu_2S Solar Cell

ALLEN ROTHWARF AND ALLEN M. BARNETT, MEMBER, IEEE

Abstract—A detailed model of the CdS–Cu_2S solar cell was used to analyze design limits of cell configurations based on present laboratory technology. The parameters controlling the short-circuit current, open-circuit voltage, and fill factor are treated. The limits for each of these factors is obtained. The results indicate that the attainable conversion efficiency of the CdS–Cu_2S solar cell extrapolating from the present processing technology is roughly 10 percent, as compared to a theoretical efficiency of 16 percent, if no losses occurred. A similar analysis for a cell using $Cd_{1-x}Zn_xS$ in place of CdS yields an attainable efficiency of 15 percent and a theoretical efficiency of over 26 percent.

The model identifies those processing parameters which must be improved in order to optimize cell efficiency. Once technology is improved, the processing parameters will be reassessed with an aim towards increasing the maximum attainable efficiency.

I. Introduction

The CdS–Cu_2S solar cell has been widely studied [1] over the last twenty years for both the interesting scientific phenomena it exhibits and its promise as a low-cost device for the direct conversion of sunlight to electricity. To succeed in producing an efficient CdS–Cu_2S solar cell it is necessary to couple fabrication techniques with a basic understanding of the device. It makes little sense to vary fabrication procedures trying to increase the conversion efficiency of a device when fundamental considerations indicate that the limits for a particular design have already been achieved. The analysis presented here for the CdS–Cu_2S cell treats the various factors which determine the short-circuit current, open-circuit voltage, and fill factor of the cell, and indicates how individual factors can be varied to achieve the optimum efficiency based on present technology. Specific results are presented for existing cells and for the next series of experiments.

The CdS–Cu_2S cells are presently made using a substrate of electroformed Cu ~ 25 μm thick which is plated with ~1 μm of Zn. CdS powder is evaporated at a source temperature of ~1000°C from a graphite source, onto the heated substrate (~300°C). Cells have been made with CdS thickness ranging from 8 to 50 μm, with typical values of 20 μm. The resistivity of the CdS layer ranges from ~0.1 to 10 Ω · cm, with 1 Ω · cm a typical value. Crystallite diameters range from 1 to 5 μm.

The Cu_2S layer is formed by dipping the CdS into a cuprous ion solution at ~90°C for 5 to 10 s. Improvements in the short-circuit current of up to 15 percent can be obtained by etching the CdS layer in HCl for ~5 s prior to forming the Cu_2S layer. The Cu_2S is on the order of 1000–3000 Å thick and formation of Cu_2S down grain boundaries to a depth of 1–2 μm can be seen in cross-sectioned samples. The resistivity of the Cu_2S is on the order of 10^{-2}–10^{-1} Ω · cm and is largely controlled by the thickness of the Cu_2O layer which forms on the surface.

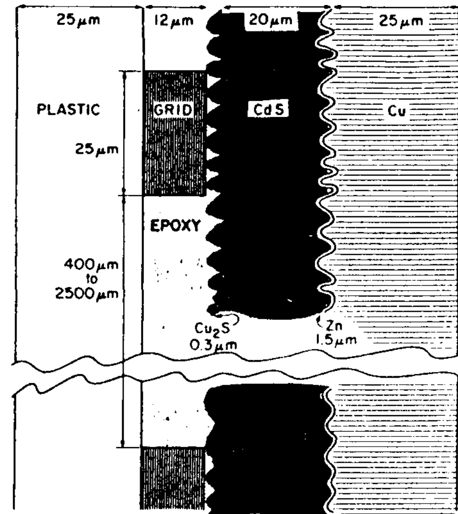

Fig. 1. Scale diagram of CdS–Cu_2S solar cell.

A gold-plated copper grid and protective plastic cover material are attached to the Cu_2S with epoxy using a lamination procedure which heats the cell to ~200°C for times ranging from 15–60 min. Further heat treatments in vacuum at 170°C for ~16 h and heat treatments in hydrogen are used as needed to obtain optimum efficiency from the cell. Fig. 1 is a scale view of such a CdS–Cu_2S solar cell.

The design changes which have taken place or are contemplated involve increased transmission of the grid, evaporated grids instead of laminated grids, anti-reflection coatings instead of etching, doping of CdS instead of source and substrate temperature variation, and use of a solid-state reaction to form the Cu_2S layer instead of the dip process. These process controls coupled with the theoretical models described below allow the cell to be designed for a predetermined efficiency.

In Fig. 2 we illustrate the band diagram which is valid for the CdS–Cu_2S cells under discussion here. Cu_2S is a degenerate or near degenerate p-type semiconductor ($p \gtrsim 10^{19}/cm^3$) with the acceptors being Cu vacancies. CdS is an n-type semiconductor due the excess Cd incorporated in its growth, with typical carrier concentrations on the order of $10^{17}/cm^3$. Hence the space-charge region exists almost entirely in the CdS layer.

Manuscript received. This work was supported in part by the National Science Foundation under Grant NSF/RANN/AER/72-03478 until July 1976 and presently by ERDA Grant E-(49-18)-2538.

The authors are with the Institute of Energy Conversion, University of Delaware, Newark, DE 19711.

Copyright © 1977 by The Institute of Electrical and Electronics Engineers, Inc.
Printed in U.S.A. Annals No. 704ED012

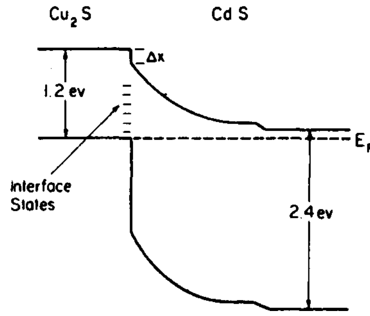

Fig. 2. Band diagram of the CdS–Cu_2S solar cell.

The basic photovoltaic behavior of the cell [2], [3] consists of the creation of electron–hole pairs in the Cu_2S layer by the absorption of photons with energy $h\nu > E_{g1}(Cu_2S)$ and the diffusion of the electrons to the Cu_2S–CdS interface. There the electrons cross into the CdS and are either swept into the CdS by the high field in the space-charge region or are trapped by interface states and recombine with holes in Cu_2S an the interface. The field at the junction is affected by the voltage across the cell, the light reaching the junction, and the distribution of donors and acceptors near the junction in CdS. These factors influence the short-circuit current and fill factor. The open-circuit voltage is largely controlled by the interface recombination process, since the forward diode current flows by this mechanism.

The maximum power output of the cell is given by the relation $P_{max} = I_{sc}V_{oc}FF$, where I_{sc} is the short-circuit current, V_{oc} the open-circuit voltage, and FF the fill factor of the cell. While these three quantities are not totally independent of one another, in the present technology they can be varied independently and represent a convenient and meaningful way of treating cell design. In more nearly optimized cells, their interdependence will become a factor limiting the ultimate achievable cell efficiency.

TABLE I
Factors Affecting Short-Circuit Current in CdS–Cu_2S Solar Cells

I. Photon Economy
  A. Reflection Losses
    1. Air-cover material Interface
    2. Cover material - Cu_2S Interface
    3. Cu_2S-CdS Interface
    4. CdS-substrate interface
  B. Absorption Losses
    1. In cover material
    2. In Cu_2S free carrier absorption
    3. In CdS
    4. In substrate
  C. Shading
    1. Grid - spacing of lines - width of lines

II. Pair Economy
  A. Generation
    1. In Cu_2S - factors of importance
      (a) Absorption coefficient $\alpha_1(\lambda)$
      (b) Mode of operation of cell-- Frontwall, frontwall reflection, backwall, backwall reflection
      (c) Thickness of Cu_2S
      (d) Spectral distribution
    2. In CdS - factors of importance
      (a) $\alpha_2(\lambda)$
      (b) $\alpha_1(\lambda)\ d_1$ i.e. light which reaches CdS in frontwall operation
  B. Collection
    1. In Cu_2S - factors of importance for electron collection
      (a) Diffusion length, $L_n = (\frac{kT}{q}\ \mu_n\tau_n)^{1/2}$
      (b) Drift field, F_1 in bulk depends on gradient in impurities or vacancies
    2. In CdS - factors of importance for hole collection
      (a) Diffusion length
      (b) Drift field near junction F_2
  C. Losses
    1. In Cu_2S - factors of importance for electron losses
      (a) Surface recombination velocity $(\frac{S\tau}{L})$
      (b) Grain boundary recombination $(r/d_1, \alpha(\lambda))$
      (c) Bulk recombination (L/d_1)
      (d) Interface recombination - (S_I, μ_2F_2)
    2. In CdS - factors of importance for hole and electron losses
      (a) Deep level density near junction in CdS
      (b) Field at junction F_2
      (c) Interface recombination

II. Short-Circuit Current

The short-circuit current in the CdS–Cu_2S solar cell is generated almost entirely (~99 percent) in the Cu_2S layer, despite the fact that this layer is only 1000–2000 Å thick in typical cells. The factors which determine the short-circuit current are summarized in Table I. We have classified the factors into those which affect the generation or loss of electron–hole pairs and those which are related to photon economy.

For short-circuit current we use the equation $I_{sc} = A_\perp j_{sc}$, with $A_\perp$ the measured area of the cell and

$$j_{sc} = \frac{\mu_2 F_2(\Phi')}{S_I + \mu_2 F_2(\Phi')} \int_{\lambda=0}^{\lambda_g} \Phi_0(\lambda) T_g [1 - R(\lambda)][1 - A(\lambda)] \times \eta_{coll}(\alpha(\lambda), L, d_1, F_1, r, S)\, d\lambda \quad (1)$$

where λ_g is the photon wavelength corresponding to Cu_2S bandgap ($\lambda_g = hc/E_{g1}$), μ_2 is the mobility in CdS; F_2 is the electric field at the junction and can be a function of the total photon flux Φ' which reaches the CdS–Cu_2S interface, S_I is the interface recombination velocity, $\Phi_0(\lambda)$ the photon flux density incident upon the cell, T_g the transmission of the grid contact, $R(\lambda)$ the effective reflection coefficient of the cell, $A(\lambda)$ the effective absorption loss coefficient of the cell, and η_{coll} the collection efficiency of the Cu_2S layer, i.e. the number of electrons per incident photon which cross the Cu_2S–CdS interface: η_{coll} depends upon the following properties [4], [5] of the Cu_2S: absorption coefficient $\alpha(\lambda)$, diffusion length $L = (kT\mu_n\tau_n/q)^{1/2}$, thickness d_1, grain size r, drift field F_1, and surface recombination velocity S. η_{coll} also depends upon the mode of operation [5] of the cell, i.e. whether the light is incident through the Cu_2S (frontwall) or through the CdS (backwall) and whether reflectors are used to reflect photons not absorbed by a single pass through the Cu_2S layer. Equations for η_{coll} and calculations for various parameter values have been reported previously [4], [5].

The factor preceding the integral in (1) is the interface collection factor and determines what fraction of electrons reaching the junction are swept into the CdS; the others

TABLE II
Factors Determining j_{sc} for AM1 Spectrum for Various Cell Designs

CdS Cells	Absorption Reflection	Grid% Shading	Surface* Loss %	Bulk Loss* Recombination	Interface* Loss	Grain* Boundary Loss	Back Surface* + Bulk CdS Light Loss	Total Losses %	j_{sc}* mA/cm²	j_{sc} mA/cm²
Dec. 1975	8	19	1	15	5	1	2	42	20	20.1
June 1976	8	9	1	15	5	1	2	35	23	22.6
Present Experiments	5	4	1	15	5	1	2	29	25	24.65
Next Generation	5	4	1	10	5	1	2	25	26	--

*Calculated quantity.

return to the Cu_2S via the interface states. The field F_2 and its dependence on voltage are determined by the intensity and wavelength of the light reaching the CdS layer near the junction as well as the compensation of this region. The quenching and enhancement effects seen in the spectral response of the short-circuit current of the cell [6]-[10] are due to this factor. The variation of F_2 with wavelength is directly related to the photocapacitance [10]-[12] of the cell.

The fact that j_{sc} depends upon F_2 which in turn depends upon the voltage across the cell, affects both the open-circuit voltage and the fill factor. We will return to this point in our treatment of the fill factor of the cell.

A number of the parameters which appear in (1) are not known with great precision, in particular, $\alpha(\lambda)$ and L are dependent upon the stoichiometry of the Cu_2S (really Cu_yS with $y > 1.99$, needed for good cells). The α, L values used in our calculations [14] are probably within a factor of two of the actual values. The values for S, F_1, S_I, and μ_2 are also only estimates.

Despite these difficulties, it is possible to make what we feel are reasonable estimates of the various terms, and predict how parameter changes will affect I_{sc}.

We estimate from various data on terrestrial sunlight, that a typically noon photon flux for $h\nu > 1.2$ eV is on the order of $2.2 \times 10^{17}/\text{cm}^2 \cdot \text{s}$. This corresponds to a lossless current density of ~35 mA/cm². In addition, measurements [13] of the photon distribution of our indoor Cu_2SO_4 filtered tungsten-iodide light source, when it has been set for AM1 simulation by use of a calibrated standard cell gives this flux within the uncertainty of the measurements, although the distribution is shifted toward the long wavelength end of the spectrum. Using 35 mA/cm² as the starting point and knowing the best currents that have been achieved for various designs, one can use theory and experiments to try to assess where these losses occur.

Reflection measurements on laminated cells, i.e. etched material with cover plastic (Aclar) and epoxy show 6 to 8-percent reflection over the spectral range of interest. The Aclar 22A plastic absorbs less than 2 percent over the range of interest. (The Aclar transmission curves show ~92-percent transmission, but with an index of refraction ~1.65, 6 percent of the loss is due to reflection.) Hence, one can assign roughly an 8 percent loss in j_{sc} to reflection and absorption losses in the cover material. To determine the grid transmission, microscope studies of the grid, as well as optical transmission have been used. The values for existing cells are listed in Table II under grid shading. The projected values are the result of considering the optimum possible grid design and are discussed more fully under fill factor.

The bulk, surface, grain boundary, and interface recombination losses are hard to decouple experimentally. The theoretical expressions, however, include these terms explicitly and estimates of individual terms can be made. Thus the interface collection factor can be estimated from photocapacitance measurements which give values for the field at the junction, and the open-circuit voltage can be used to estimate S_I, and resistivity and capacitance to estimate μ_2. The results of this analysis give 5 percent as a representative loss due to the interface recombination path.

Expressions for grain boundary losses as function of Cu_2S thickness, absorption coefficient, and grain size have been derived and evaluated [14], [15]. The conclusion reached from these studies is that grain boundary recombination is not a significant factor in present forms of the CdS-Cu_2S cell. This results from a number of factors including the extreme thinness of the Cu_2S layer, and the way in which the Cu_2S is formed on the polycrystalline CdS. We have thus assigned a 1-percent loss to this cause in Table II.

The bulk and surface recombination losses have been treated theoretically by calculating the collection efficiency η_{coll} as a function of $\alpha(\lambda), d_1, F_1, S, L = (kT\mu_1\tau/q)^{1/2}$, and the modes of operation of the cell. The expressions have been evaluated [4], [5] for various values of αL, αd, F_1 and S_T/L, and compared with experimental spectral response curves. Experimental values for $\alpha(\lambda)$, L, and d_1 on our materials are uncertain by a factor of two or more, and for F_1, the

drift field, and S the surface recombination velocity no measurements have been attempted. For reasonable values of the parameters, however, the results show that bulk recombination losses in the Cu_2S are on the order of 15 percent, and surface recombination losses are not significant. A rationale for this last statement can be found in the fact that a few monolayers of Cu_2O exist on the Cu_2S. This layer should act to passivate the surface and reduce surface losses. We have thus indicated 1-percent surface losses and 15-percent bulk losses in Table II.

One additional loss factor is listed in Table II. This factor is photon losses in CdS and at the back surface of the cell. Its magnitude is related to the absorption coefficient of the CdS for below bandgap radiation and the reflection coefficient of the back surface material, which in our case is zinc-plated copper. The magnitude of this factor is also dependent upon the thickness and absorption coefficient of the Cu_2S, since in the front wall operation of the cell only light which passes through the Cu_2S is subject to such losses.

In our picture of the operation of the cell some of this loss is unavoidable. The light incident upon the cell is only partially absorbed in its initial pass through the Cu_2S, since for $d_1 > L/2$, electron losses in the bulk become too large. Experiments on cells with transparent substrates [5] have shown increases in current of 20 percent or more when a good mirror replaced a total absorber under the cell. Reflected light from the substrate thus represents a substantial part of the cell response, particularly for long wavelengths. Due to the high index of refraction of the Cu_2S ($n > 3$), and the rough texture of its surfaces most of the light reflected from the substrate and not completely absorbed in the second pass through the Cu_2S, is totally internally reflected. The 2-percent loss value indicated in Table II is estimated from the above considerations.

The expected short-circuit current is obtained from the product $j_{sc} = 35\ \Pi_i(1 - l_i)$, with the l_i the decimal losses indicated in Table II.

The loss for each mechanism in Table II depends upon specific material parameters, i.e. surface treatment, Cu_2S carrier concentration, CdS carrier concentration, grain size, etc. We have varied these parameters and found the resulting changes in cell properties to be in agreement with the predictions of our analysis. The cell improvements achieved so far were as expected, and the present experiments attacking other key loss areas are also yielding expected improvements.

III. Open-Circuit Voltage

The open-circuit voltage of the cell can be explained using the interface recombination model of the cell [3]. Based upon this model the current in the cell is given by

$$I = qA_jN_{c2}S_I \exp\left[-(E_{g1} - \Delta X)/kT\right] \times \{\exp\left[q(V - IR_s)/kT\right] - 1\} - A_{\perp}j_{sc} \quad (2)$$

where q is the electronic charge, A_j the junction area (which can be many times larger than the normal area of the cell, due to formation of Cu_2S in CdS grain boundaries), N_{c2} ($\sim 2 \times 10^{18}$ cm^{-3}) the effective density of states at the band edge of the CdS, S_I the interface recombination velocity which depends upon the lattice mismatch Δa between Cu_2S and CdS (with $\Delta a/a = 0.04$ an estimate [3] for S_I is 10^6 cm/s); E_{g1} is the bandgap of $Cu_2S \sim 1.2$ eV, ΔX the difference in electron affinity between Cu_2 and CdS ~ 0.2 eV (see Fig. 1), V the applied voltage or load voltage, and R_s the series resistance of the cell. The shunt resistance of the cell has been assumed to be so large that a term $(V - IR_s)/R_{sh}$ has been dropped from (2).

From (2) for $I = 0$ we can write, for $qV_{oc} \gg kT$,

$$qV_{oc} = E_{g1} - \Delta X + kT \ln j_{sc} - kT \ln qN_{c2}S_I - kT \ln A_j/A_{\perp} \quad (3)$$

where we have neglected the variation of j_{sc} with field.

To improve the open-circuit voltage of the cell, based on (3) the parameters subject to change are ΔX, S_I, and A_j. Since ΔX and S_I are directly related to fundamental material properties, they can only be changed significantly by changing materials. This has been accomplished [16]–[18] by the use of $Cd_{1-x}Zn_xS$ in place of CdS, with the result that open-circuit voltages on the order of 0.7 V have been reached [17], [19]. The main cause of this increased voltage is the decrease in ΔX, which has been verified by studies of the saturation current [19], and spectral response versus photon energy [19]. The other factor which can be modified is the junction area A_j. By forming a planar junction instead of the highly convoluted one which occurs in present polycrystalline cells, an increase in V_{oc} by as much as 0.06 V can be expected. Formation of Cu_2S on evaporated CdS using a dry process (deposition of Cu_2Cl_2) has produced cells [19] with $V_{oc} \sim 0.54$ V. This results from a reduction in junction area, since Cu_2S no longer forms in grain boundaries. A further increase in V_{oc} by $\sim$0.03 V would be expected if single crystal CdS were used; this would reduce the junction area by a factor of $\sim$3 by eliminating the topological roughness associated with the evaporation of CdS on rough Cu, and the etching of the CdS. Data [1] on single crystal cells show V_{oc}'s as high as 0.6 V, but for unspecified intensities. Since the use of single crystal CdS is impractical from cost considerations, and etching provides beneficial antireflection properties, a V_{oc} value of 0.54 V is the design goal of pure CdS cells.

The quantities in (3) are obtainable from experiment. $(E_{g1} - \Delta X)$ can be evaluated by several independent techniques. The first uses current–voltage curves at various temperatures in conjunction with (2) to obtain the saturation current $j_0 = qA_jN_{c2}S_I \exp\left[-(E_{g1} - \Delta X)/kT\right]$ from the intercept of $\ln (I + I_{sc})$ versus V, and then the slope of $\ln j_0$ versus $1/kT$ gives $(E_{g1} - \Delta X)$. From (3) a plot of V_{oc} versus kT gives $(E_{g1} - \Delta X)$ as the $T = 0$ intercept [11]. A third method is by plots of $(j_{sc})^{1/2}$ versus photon energy from the spectral response measurements [11]. The three methods are in substantial agreement and yield $(E_{g1} - \Delta X)_{max} \simeq 1$ eV.

The quantity $qA_jN_cS_I$ was obtained from the intercept of the $\ln j_0$ versus $(kT)^{-1}$ line, while $A_j/A_{\perp}$ was estimated

TABLE III
Evaluation of Quantities Determining Open-Circuit Voltage for Various Cell Designs

CELL	$E_{g1} - \Delta X$	$+kT \ln j_{sc}$	$-kT \ln qN_{c2}S_I$	$-kT \ln A_j/A_\perp$	Calculated V_{oc}
DEC. 1975 CdS	1.0	-0.1	-0.33	-.06	.51
JUNE 1976 CdS	1.0	-0.1	-0.33	-.06	.51
PRESENT CdS EXPERIMENTS	1.0	-0.1	-0.33	-.06	.51
CdS NEXT GENERATION	1.0	-0.1	-0.33	-.03	.54
$Cd_{1-x}Zn_xS$ PRESENT EXPT.	1.2	-0.1	-0.33	-.06	.71
$Cd_{1-x}Zn_xS$ NEXT GENERATION	1.2	-0.1	-0.33	-.03	.74

from studies of the equivalent Cu_2S thickness (determined chemically) coupled with either the depth of Cu_2S penetration down grain boundaries, or the midgrain Cu_2S thickness [14]. The variation of V_{oc} with "dip time", when the Cu_2S layer is formed by the wet process can also yield estimates of $A_j/A_\perp$.

The net effect of this analysis is that for the cells under discussion here, $(E_{g1} - \Delta X) \simeq 1$ eV, $S_I \simeq 10^6$ cm/s, $A_j/A_\perp \simeq 10$, and $V_{oc} \simeq 0.51$ V in typical present day cells.

In Table III we have indicated the magnitude of the terms in (3) which enter into the determination of V_{oc} for various past, present, and future solar cell designs.

There are other factors which can affect V_{oc}. In particular, if a drift field exists in the Cu_2S layer, or the doping level in CdS becomes too high, some of the diffusion voltage will appear in the Cu_2S and lower V_{oc}. Such affects would also alter the diode factor, i.e. q/kT in the exponents in (2) is replaced by q/AkT with $A > 1$. These effects can be eliminated by maintaining $p > 10^{19}/\text{cm}^3$ in Cu_2S and $n \simeq 10^{17}/\text{cm}^3$ in CdS.

IV. Fill Factor

Since the fill factor is defined in terms of the maximum power point, i.e. $FF = V_{mp}I_{mp}/V_{oc}I_{sc}$, it is determined by maximizing the product $P = |I|V$ using (2). The resulting implicit function can be solved numerically. For small series resistance ($R_s \ll V_{oc}/I_{sc}$) a linearized expression is obtained:

$$FF = FF_0\left(\frac{qV_{oc}}{kT}\right) - \frac{I_{sc}R_s}{V_{oc}}C\left(\frac{qV_{oc}}{kT}\right). \qquad (4)$$

In Fig 3, FF_0 and C are plotted as a function of V_{oc}, for $T = 300$ K. For $V_{oc} = 0.51$ V, $FF_0 = 0.80$, and $C \doteq 0.90$.

The contributions to R_s in the cell are primarily due to the lateral flow of current in the thin Cu_2S layer, and the resistance of the CdS layer, in particular the compensated region of the CdS near the junction. The resistance due to the grid material can also contribute, but in cells studied so far it is not significant. Since the series resistance due to the Cu_2S layer depends on the spacing of the grid wires S, ($R_1A_\perp = \rho_1 S^2/12d_1$, with 1 referring to Cu_2S, d_1 is the thickness and ρ_1 the resistivity of the layer), and the transparency of the grid T_g is also dependent on the grid

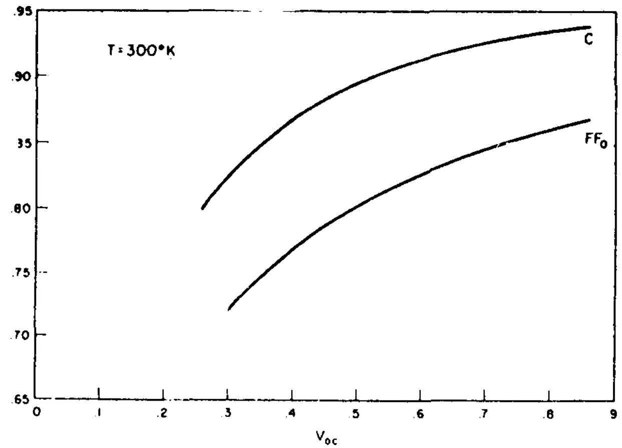

Fig. 3. Plots of calculated values of ideal fill factor and multiplicative factor in (4), as a function of open-circuit voltage.

spacing, i.e. for a parallel line grid $T_g = S/(S + \delta)$ where δ is the grid line width, one can obtain an expression for the grid spacing which gives highest efficiency [20]. One maximizes the product T_gFF and obtains the relation (for $\delta/S \ll 1$).

$$S \simeq \left[\frac{6V_{oc}}{Cj_{sc}}\frac{d_1}{\rho_1}\,\delta\left(FF_0 - C\frac{j_{sc}}{V_{oc}}R_2A\right)\right]^{1/3} \qquad (5)$$

where R_2 is the series resistance other than that due to Cu_2S. The value of δ is determined by the state of the art in the technology used to apply the grid. For the CdS–Cu_2S cell with both evaporated and gold-plated grids $\delta \simeq 20$ μm, and $\rho_1/d_1 \simeq 10^3$–10^4 Ω. For these values one can obtain transparency values in the 0.94 to 0.97 range, and reductions in fill factor due to the Cu_2S of 0.015 to 0.035.

In actual cells the reduction in fill factor from the ideal FF values ranges from 0.05 to 0.1 or more. Part of this arises from the $R_2A_\perp$ component which is primarily due to a compensated layer in CdS near the junction; it has an effective resistivity ρ_2^* and width d_2^*. This reduces FF by $Cj_{sc}\rho_2^*d_2^*/V_{oc}$. The values of $\rho_2^*d_2^*$ are dependent upon the heat treatments received by the cell. The magnitude of d_2^* is related closely to the "cross-over" phenomena [1], [2] between the dark and light I–V curves, which is seen when the curves are obtained by a voltage sweep. If sufficient time is given in the dark for steady-state current to be achieved, the dark and light curves are very nearly the same except for the displacement along the I axis by I_{sc}. For typical cells the reduction in FF due to the compensated region can be on the order of 0.01 or greater depending upon the extent of its heat treatment, the longer the heat treatment the larger the reduction in FF.

Another contribution to loss in fill factor which is also related to the heat treatments and the existence of the compensated layer is that due to the voltage dependence of interface collection factor. As mentioned earlier in (1) the factor preceding the integral depends upon voltage and makes j_{sc} appearing in (2) voltage dependent. While this dependence is expected to have a negligible effect on V_{oc}, due to the logarithmic dependence, it can seriously affect

the fill factor, since the current at the maximum power point is directly dependent upon j_{sc} and hence F_2.

The field at the junction in the light can be broken into two components, one which is independent of voltage but dependent upon the wavelength and intensity of the light, and the other which is voltage dependent. In essence in the CdS layer close to the junction the compensating centers are ionized, producing an increase in the positive charge density close to the junction, and hence reducing the width of the space-charge region needed to support the diffusion voltage V_D^*. It is this reduction in space charge width which accounts for the marked increase in cell capacitance produced by light [10]–[12]. The field at the junction is also increased over the field in the dark, since the net charge is increased. The component of the field resulting from the ionization of the compensating centers is essentially independent of voltage, while the field resulting from the remaining space charge is voltage dependent. We can write

$$F(V) = F_{light} + [2(V_D^* - V)qN_D^*/\epsilon\epsilon_0]^{1/2}$$

where F_{light} is the field resulting from the ionization of the compensating centers by light, V_D^* is part of the diffusion voltage which is supported by the remaining space charge, and N_D^* is the net donor concentration $(N_D - N_A)$ in the compensated region. The larger F_{light}, the smaller V_D^* and the smaller the voltage dependence of $F(V)$ and hence of j_{sc}. The values of N_D^*, F_{light}, and V_D^* are not known precisely, and vary with heat treatment. In addition, μ_2 and S_I are only known approximately. However, one can estimate that the change in FF due to this cause is on the order of 0.01 to 0.03. If the compensated region did not exist, changes in FF due to this mechanism would be on the order of 0.02 to 0.06. This is consistent with the observation that heat treatments initially lead to an improvement in fill factor.

A further mechanism for loss in fill factor is the shunt resistance of the cell. Its behavior is similar to the voltage dependent j_{sc} term treated above in that the current at the maximum power point is reduced; the reduction in I_{mp} is roughly V_{mp}/R_{sh}. Hence the reduction in FF due to this cause is given by

$$\Delta FF = \frac{V_{mp}}{I_{sc}R_{sh}} = \frac{V_{mp}}{j_{sc}A_\perp R_{sh}}.$$

In good cells $R_{sh}A_\perp > 1000$ and $\Delta FF < 0.02$.

A similar analysis holds for the $Cd_{1-x}Zn_xS - Cu_2S$ solar cell. However, due to its higher V_{oc}, its fill factor as indicated by Fig. 2 will be higher by 5 percent, than that of the $CdS-Cu_2S$ cells. In Table IV the calculated fill factors of past, present, and future cell designs are given.

V. Efficiency

Since the conversion efficiency of the cell is defined as P_{max}/P_{in} with P_{in} the total light input, we can obtain it by the relation $\eta = V_{oc}I_{sc}FF/P_{in}$. For terrestrial considerations, AM1 for P_{in} has been used for lack of a true standard. The value of P_{in} used in this case is 0.1 W/cm^2 = 1 kW/m^2. Hence $\eta = V_{oc}j_{sc}FF$; with j_{sc} in mA/cm^2, η is a percentage. In Table V we list the expected efficiencies for $CdS-Cu_2S$ and $Cd_{1-x}Zn_xS-Cu_2S$ cells for the values of j_{sc}, V_{oc}, and FF discussed in this analysis.

TABLE IV
Calculated Fill Factor Reduction Terms for Various Cell Designs

	Series Resistance Cu_2S	Series Resistance CdS	Field Effect	Net Fill Factor
Dec 1975 CdS	-0.04	-0.04	-.03	0.69
June 1976 CdS	-0.02	-0.04	-.03	0.71
Present CdS Experiments	— .02	-0.02	-.03	0.73
CdS Next Generation Planar	-0.02	-0.02	-.03	0.74
$Cd_{1-x}Zn_xS$	-0.02	-0.02	-.03	0.77
$Cd_{1-x}Zn_xS$ Planar	— .02	- 0.02	-.03	0.78

TABLE V
Conversion Efficiency Calculations for Various Cell Designs

Cell	j_{sc} (mA/cm^2)	V_{oc}	FF	η%
CdS No Losses	35	0.57	0.81	16.1
CdS Dec 1975	20	0.51	0.69	7.1
CdS June 1976	23	0.51	0.71	8.3
CdS Present	25	0.51	0.73	9.3
CdS Next Generation	26	0.54	0.74	10.4
$Cd_{1-x}Zn_xS$ No Losses	35	0.77	0.85	23
$Cd_{1-x}Zn_xS$ Goal Present	20	0.71	0.77	10.9
$Cd_{1-x}Zn_xS$ Next Generation	26	0.74	0.78	15.0

We note in passing that the ideal efficiency of the $Cd_{1-x}Zn_xS$ cell was calculated under the assumption that even after the electron affinity difference with Cu_2S is eliminated by proper choice of x, the dominant current mechanism in the cell is still interface recombination. If the dominant current mechanism becomes bulk recombination in Cu_2S, then the possible room temperature value of V_{oc} increases to 0.86 V, FF_0 to 0.86, and η to 26 percent, using present estimates for $\tau(10^{-9}$ s) and $L(3 \times 10^{-5}$ cm) in Cu_2S.

The histogram in Fig. 4 shows the limits of design and the goals of experiments (95 percent of limit of design) for past, present, and future cells. The goals of the experiment have been achieved for December 1975 and June 1976 designs.

VI. Discussion

We have tried to indicate in this paper in some detail the major factors which determine the performance of the $CdS-Cu_2S$ and the $Cd_{1-x}Zn_xS-Cu_2S$ solar cells. A number

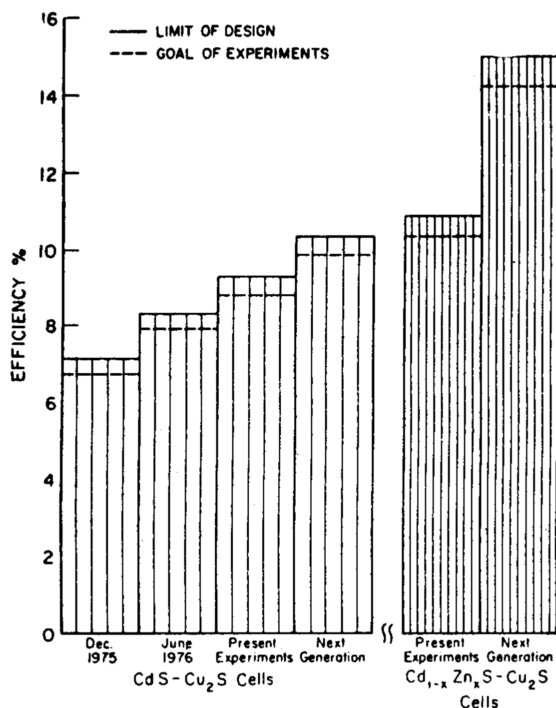

Fig. 4. Efficiency-design histograms. Goals have been reached for December 1975 and June 1976 designs.

of fine details have been omitted for lack of space and because they have been treated elsewhere [3]–[5], [14], [15]. The model we have used to obtain present cell characteristics and predict future performance, is a straightforward application of standard semiconductor physics, which holds for the $CdS–Cu_2S$ cell and other p-n junctions. From its discovery right through to the present, rather exotic models [21], [22] have been invoked to explain the operation and various characteristics of the $CdS–Cu_2S$ cell. We on the other hand have found that while many factors are involved in understanding the cell and controlling its properties, they are all rather prosaic and can be treated simply.

The projected conversion efficiency for an optimized $CdS–Cu_2S$ cell, based on present technology is somewhat over 10 percent, while that for an optimized $Cd_{1-x}Zn_xS–Cu_2S$ cell is over 15 percent. While these figures may seem optimistic, and simply a repetition of what has been said before, these numbers are not theoretical upper limits but rather design goals, i.e. if we give theoretical no loss estimates, the upper limits for efficiency become 16 percent for the $CdS–Cu_2S$ cell. and 26 percent for the $Cd_{1-x}Zn_xS–Cu_2S$ cell.

It is obvious that when present experimental goals have been met a reassessment will be made of the factors determining the cell efficiency. Any technological innovations will be incorporated and a new design goal set.

REFERENCES

[1] A. G. Stanley, *Applied Solid State Sci.*, vol. 5. New York: Academic Press, 1975, pp. 251–366, (contains a review of $CdS–Cu_2S$ research through 1973, with nearly 500 references).
[2] L. R. Shiozawa *et al.*, Clevite Final Report ARL 69-0155, Oct. 1969.
[3] A. Rothwarf, International Workshop on Cadmium Sulfide Solar Cells and Other Abrupt Heterojunctions, University of Delaware, May 1975, NSF-RANN AER 75-15858, pp. 9–50.
[4] A. Rothwarf, NSF/RANN/AER 72-03478 A03/TR 75/3, May 1975.
[5] A. Rothwarf *et al.*, in Conference Record Eleventh IEEE Photovoltaic Specialists Conference, May 1975, p. 476.
[6] N. Duc Cuong and J. Blair, *J. Appl. Phys.*, vol. 37, p. 1660, 1966.
[7] A. E. Potter and R. L. Schalla, in *Rec. 6th IEEE Photovoltaic Spec. Conf.*, 1967, p. 24.
[8] A. E. Potter *et al.*, in *Rec. 7th IEEE Photovoltaic Specialists Conf.*, 1968, p. 62.
[9] W. D. Gill and R. H. Bube, *J. Appl. Phys.*, vol. 41, p. 3731, 1970.
[10] P. F. Lindquist, Ph.D. dissertation, Stanford University, 1970.
[11] J. Lindmayer and A. G. Revesz, *Solid-State Electronics*, vol. 14, p. 647, 1971.
[12] P. F. Lindquist and R. H. Bube, *J. Appl. Phys.*, vol. 43, p. 2839, 1974.
[13] H. C. Hadley, Jr., NSF/RANN/SE/GI 34872 TR74/3.
[14] A. Rothwarf, in *Proceedings of International Conference on Solar Electricity*, (Toulouse, France, Mar. 1976); also NSF/RANN/AER 72-03478 A04/TR 76/1, Mar. 1976.
[15] A. Rothwarf, in *Conf. Record 12th IEEE Photovoltaic Spec. Conf.* (Nov. 1976).
[16] W. Palz *et al.*, in *Rec. 10th IEEE Photovoltaic Spec. Conf.*, 1973, p. 69.
[17] L. C. Burton and T. L. Hench, *Appl. Phys. Lett.*, vol. 29, p. 612, 1976.
[18] T. M. Peterson, Ph.D. dissertation, University of California, Berkeley, 1975.
[19] Progress Reports NSF/RANN/AER 72-03478/A04/PR76/1, 2.
[20] P. A. Crossley, G. I. Noel, and M. Wolf, Final Report NASW 1427, June 1968.
[21] A. E. Van Aerschodt *et al.*, *IEEE Trans. Electron Devices*, vol. ED-18, p. 471, 1971.
[22] K. W. Böer, *Phys. Rev.*, vol. B13, p. 5373, 1976.

Appendix C

PROGRESS IN THE DEVELOPMENT OF HIGH EFFICIENCY THIN FILM CADMIUM SULFIDE SOLAR CELLS*

A. M. BARNETT, J. D. MEAKIN, A. ROTHWARF

Institute of Energy Conversion
University of Delaware
Newark, Delaware 19711

Summary

Thin film photovoltaic cells of cadmium sulfide/copper sulfide have been developed and optimized for specific cell designs. The optimization has been achieved by changing material parameters and the technology of the electrical contacts as dictated by detailed analyses of loss mechanisms in the cells. Additional design changes are needed to further increase the energy conversion efficiency in direct sunlight beyond the present value of 8.5%. The application of analytic techniques to specific cell designs is responsible for the improvements achieved to date, and it is expected to lead to a basic cadmium sulfide/copper sulfide cell with an efficiency over 10%.

It is anticipated that the application of similar analytic techniques to a modified cell of cadmium-zinc sulfide/copper sulfide, coupled with constant interplay between theoretical and experimental results will lead to an energy conversion efficiency in direct sunlight of up to 14%.

The material properties and electro-optical characteristics of the present high efficiency CdS/Cu_2S cells and initial results using the mixed cadmium zinc sulfide will be presented. This paper describes the analysis driven technology innovations which have led to the development of reproducible thin film cadmium sulfide solar cells with energy conversion efficiencies in direct sunlight of greater than 8.5%.

*This work was supported in part by the National Science Foundation under Grant NSF/RANN/AER72-03478 and by the Energy Research and Development Administration under Grant E(49-18)-2538.

1. INTRODUCTION

A photovoltaic effect in CdS was first reported by Reynolds for a junction made by depositing a thin film of copper on a cadmium sulfide film (1). Later work established that the actual junction was between CdS and Cu_2S (2). A substantial number of research efforts have since been conducted on this photovoltaic heterojunction and although some variation exists, cells have generally been made by reacting a vapor deposited cadmium sulfide film with a cuprous ion solution. A major research effort aimed towards space applications was conducted during the 1960's (3,4). These and many other investigators have reported conversion efficiencies in sunlight of between 5 and 6% with a limited number reporting efficiencies up to 7%.* Thin film cells with energy conversion efficiencies of 7.8% when measured in direct sunlight were recently reported (5,6). The methodology and experiments which lead to the further development of 8.5% CdS/Cu_2S cells follows.

2. METHODOLOGY

The methodology is based on loss minimization; i.e., selective identification, analysis, and amelioration of those factors which cause the power output to fall below the ceiling set by available insolation. By use of this procedure, it is shown that cell design is primarily governed by the physical parameters of the material chosen for the "absorber-minority carrier generator," secondarily influenced by the parameters of the material chosen for the "majority carrier converter-collector" and virtually independent of the overall device configuration or structure.

The application of this loss minimization technique was the basis for the experiments which led to the improvements in energy conversion efficiency, measured in direct sunlight, of the CdS-based thin film photovoltaic cell.

Figure 1 illustrates the cell configuration that has been in use for this type of solar cell for the last fifteen years. This technology utilizes a metal substrate, evaporated cadmium sulfide, copper sulfide

---

*Shirland and Bogus and Mattes have reported efficiencies under simulated conditions above 8% (7,8). Shirland subsequently reported that the simulator measurement was probably 14.5% too high (9). Bogus and Mattes measured efficiencies under simulated space conditions (AMO) up to 8.1%; previous independent simulator tests for AMO confirmed cells of efficiencies up to 7.0%.

(formed by reaction with a cuprous ion solution), and a pressure bonded grid for electrical contact (3,4).

Based on this technology, the group at the University of Delaware achieved average efficiencies of almost 5% in early 1975 (11). By December of 1975, the average efficiency had increased to almost 6% in sunlight, but more importantly, the efficiency distribution curve was skewed to the high efficiency limit of 6.8% (12). These skewed data indicated that the materials and processes had been optimized for this solar cell design and using these experimental results, the basic loss mechanisms were analyzed to determine design changes which had to be made to raise the efficiency beyond 6.8% (5).

3. ANALYTICAL RESULTS

CdS/Cu_2S Cell

The design limits for the conversion efficiency η, short circuit current j_{sc}, open circuit voltage V_{oc}, and fill factor FF of various cell configurations based on the current laboratory technology have been published (5). An update of this analysis using recently measured parameters is given in Tables I, II, and III. Most of the parameters can be independently measured and it is these measurements which lead to the changes in goals and targets for the next generation of cells.

All laboratory experiments are aimed at achieving 95% of the design limit and this has been reached for the March 1977 generation. The goal of the current experiments is to develop a cell which is within 5% of the design limit designated in the tables as the present generation and subsequently to develop the next generation cell with more than 10% efficiency.

Open Circuit Voltage

From theoretical considerations, a significant increase in V_{oc} can be expected if the highly textured junction characteristic of the March 1977 cell generation is replaced by a smoother junction of less effective area (5). Such junctions have been obtained by forming the Cu_2S on evaporated, unetched CdS using a solid state reaction between evaporated CuCl and CdS. The resulting junction follows the untextured surface contours and does not penetrate down the CdS grain boundaries.

Cells with V_{oc} = 0.54 V have been produced in this way consistent with a junction area reduction factor of ∿ 1/3.

Short Circuit Current Density

A major factor determining j_{sc} is the photon loss due to reflection at the outer Cu_2S surface (5). Estimates of this loss for several cell designs are shown in Table I.

The low reflectance of the March 1977 cell is due to the textured Cu_2S layer and an SiO anti-reflection layer. Reflection measurements show that the total reflection loss after eliminating the texturing (in order to increase V_{oc}) is between 12 and 15%. However, calculations indicate that the total photon losses can be reduced back to about 4% by the use of more effective anti-reflection techniques than a single layer of SiO.

Some improvement in j_{sc} can be expected in the present design by optimizing the reflectance at the substrate but a major reduction of losses during the second light pass through the cell can only be achieved by a coupled optimization of Cu_2S and CdS thickness and substrate reflection. This is the basis of the next generation cell design.

Fill Factor

The increase in the fill factor (FF) design limit from 0.71 to 0.74 for the next generation cell results from the increase in V_{oc} and reductions in losses due to Cu_2S resistivity and field effects.

The FF values achieved in present high efficiency cells are somewhat lower (∿ 0.67) than the March 1977 design limit. Several factors may be contributing. Analysis of the variation of FF with spectral content has shown that voltage dependence of the interface collection factor is significant. This voltage depencence is caused by the behavior of compensating centers in the junction region. Control over the relevant centers will be sought by controlling the compensation of the CdS using appropriate heat treatments. Other possible causes of FF reduction could be the presence of light sensitive Au/CdS barriers at defects in the Cu_2S layer and various grid irregularities.

It is clear that the CdS/Cu_2S cell can exceed 10% efficiency with the enhanced V_{oc} from a planar junction. Technology must be developed to give net photon losses at or below the current levels. Refinement of techniques to control the collection field in the CdS depletion region and

the various resistive losses should bring the fill factor close to 0.74.

The next cell generation is predicted to have a design limit of 11.6%.

4. EXPERIMENTAL RESULTS

Upon completing the initial cell analysis, it was concluded that the major loss which could be eliminated occurred at the front contact where only 81% of the incident radiation was being transmitted. It appeared that this loss could be reduced by the simple engineering change of using a grid with wider spacing and narrower lines. In particular, it was calculated that a grid with 95% transmission should give about a 17% increase in current and hence in efficiency.

Such a grid was made and applied to cells that would have had efficiencies of about 6.5% with the previous, less transparent grid. The predicted increase in efficiency was not observed. Even though the short circuit current increased as expected, the fill factor degraded. The series resistance responsible for this degradation was higher than could be accounted for by the smaller geometric contact area of the new grid (only one quarter that of the original grid). It was found that the new grid failed to make contact to the Cu_2S over a significant fraction of the grid area.

To get better contact with a grid of this high transparency, gold was evaporated onto the Cu_2S through a suitable mask. However, cells with these evaporated grids had very low shunt resistances, suggesting that there were areas with direct contact between the gold and the underlying CdS layer. It was subsequently determined that this direct contact was occurring largely at the current collecting tab region of the cell which makes up the majority of the deposited gold area (See Figure 2).

To overcome the problems associated with these two grid systems, a hybrid grid system was developed which is a combination of the two. Gold grid lines were first evaporated to give good contact to the Cu_2S, but without the current collection tab to prevent the low shunt resistance. Following evaporation, a pressure bonded grid was laminated over the evaporated grid (in an orthogonal configuration) for good current collection. This hybrid system had about a 5% loss in optical transmission over that of a single high transparency grid, but it did result in the

predicted increase in efficiency of the cells.

Figure 3 shows the distribution of efficiencies for 24 cells produced during June 1976 with the grid configuration described above. The average efficiency is over 6.8% and the maximum efficiency achieved during June was 7.64% in an actual rooftop test. During July a further improvement in maximum efficiency to 7.77% was achieved, Figure 4. Cross checking with the NASA-Lewis Research Center's test facility has validated these reported efficiency measurements (13).

The distribution in Figure 3 is again skew, indicative of a design limit. There are still significant losses from optical transmission of the grid which is only 91% for this hybrid grid design. The June 1976 cell design results in absorption and reflection losses at the cover plastic and Cu_2S surface totaling 8%, in addition to the 9% loss from the hybrid contact system.

The hybrid grid structure was intended as an interim measure, and subsequently cells have been developed using an all-evaporated grid of 95% transmission with the addition of a single layer SiO anti-reflection coating. As can be seen from Table I, this should give about a 10% increase in current and a corresponding increase in cell efficiency. The problems with shunting caused by the current collection tab have been overcome by laying down a 25 μm thick insulating layer underneath the tab. The design efficiency for this cell is 9.1% and an actual conversion efficiency of 8.55% has now been reached. The I-V curve for this cell is shown in Figure 5.

The efficiency achieved with the 9.1% cell design (March 1977, Table III) is sufficiently close to the design limit to mandate a change to the next type of cell (present cell, Table III). The design should give a slightly higher current, but the most significant advance expected is in open circuit voltage. The cells made so far have all had open circuit voltages of ∿ 0.50 V. This is largely determined by the electron affinity mismatch between the Cu_2S and the CdS, which reduces the achievable voltage by 0.2-0.3 V. As previously mentioned, the elimination of surface texturing and grain boundary Cu_2S reduces the actual junction area and results in open circuit voltages up to 0.54 V. There is a short circuit current penalty caused by not etching the CdS, as the front surface reflection is then markedly increased and light trapping after reflection from

the substrate no longer takes place. To maintain the enhanced open circuit voltage and simultaneously generate high short circuit currents, the development program is now focusing on the use of a single or double layer antireflection coating to bring the front surface reflection back down to about 5%. The present design is calculated to have a conversion efficiency limit of 10%. Further reductions in the photon losses due to absorption in the CdS and metal substrate, combined with improvements in fill factor, should give an ultimate design efficiency of over 11%, which means that actual cells of over 10% efficiency will be producible.

5. MODIFIED SOLAR CELLS BASED ON CdS/Cu_2S

The use of the CdS/Cu_2S heterojunction is in large part a historical accident. Measurements of the barrier height to reverse electron flow show that the electron affinity mismatch between the two components is between 0.2 and 0.3 V, which directly reduces the achievable open circuit voltage. The Cu_2S bandgap of 1.2 eV should in fact allow the development of an open circuit voltage of between 0.7 and 0.8 V. The electron affinity of the n-type side of the junction can be changed by using a solid solution of CdS and ZnS. At about 20% Zn the electron affinities of the mixed sulfide and the Cu_2S are matched and open circuit voltages above 0.7 V should be achievable. If the electric field in the mixed sulfide can be tailored to give good current collection, and the Cu_2S layer can be produced and maintained on the mixed sulfide in its high efficiency form, the achievable cell efficiency should be in excess of 15%. An active development effort is now underway on the mixed sulfide cell and is beginning to show promise of meeting the above goal. The first cells made had very low short circuit currents but the expected higher open circuit voltages were achieved. In the course of the last year, the short circuit currents have been raised progressively from the initial 10 mA/cm^2 to the present values in the 15-16 mA/cm^2 region. The current voltage characteristics of two of the best cells to date are shown in Figure 6.

The mixed sulfide layers first deposited were of high resistivity, resulting in low electric fields in the region of the junction and hence poor current collection. A concentric evaporation source has now been developed for the simultaneous evaporation of CdS and ZnS in the desired ratio (14). The evaporation temperature largely controls the film resistivity and the source design now produces film of the desired resistivity,

1-10 Ω-cm, at usable deposition rates of 0.5-3 μm/minute. Not all of the efficiency-improving design features developed for the CdS/Cu_2S cell such as high transmission grids and antireflection coatings have yet been applied to the mixed sulfide cell. During the coming year, it is expected that the mixed sulfide cells will equal the efficiency of the best CdS cells, with both types exceeding 10% conversion efficiency. Within the next two years, the mixed sulfide cell should become the most efficient type, with energy conversion efficiencies well in excess of 10%.

6. CONCLUSIONS

A detailed quantitative loss analysis of the CdS/Cu_2S cell has resulted in specific efficiency goals. A research and development effort directed by this analysis has already achieved significantly enhanced cell efficiencies and production reliability. Continued analysis-driven cell development is expected to produce thin film polycrystalline cells with a conversion efficiency in excess of 10%. The cells developed in the laboratory will provide the model for the development of a low cost thin film polycrystalline cell for widespread terrestrial application.

7. ACKNOWLEDGMENTS

The experimental and theoretical work reported in this paper has been performed by the photovoltaic group at the Institute of Energy Conversion of the University of Delaware.

References

1. D. C. Reynolds, G. M. Leies, L. L. Antes and R. E. Marburger, Phys. Rev., Vol. 96, 533 (1954). D. C. Reynolds and G. M. Leies, Elec. Eng., Vol. 73, 734, (1954).

2. W. R. Cook, Jr., L. Shiozawa and F. Augustine, J. Appl. Phys., Vol. 41, 3058 (1970).

3. A. G. Stanley, Applied Solid State Science, 5, 251-366, Academic Press 1975. A review of CdS/Cu_2S research through 1973.

4. L. R. Shiozawa, F. Augustine, G. A. Sullivan, J. M. Smith III, W. R. Cook, Jr., Clevite Final Report ARL 69-0155, Oct. 1969.

5. A. Rothwarf and A. M. Barnett, IEEE Trans. (Devices) Vol. ED-24, 381, 1977.

6. A. M. Barnett, W. E. Devaney, G. M. Storti and J. D. Meakin, IEEE

Trans. (Devices), To be published 1977.

7. F. A. Shirland, The Thin Film CdS Solar Cell, Fifth IEEE Photovoltaic Specialist Conference, 1965.

8. K. Bogus and S. Mattes, High Efficiency Cu_2S-CdS Solar cells with Improved Thermal Stability, Ninth IEEE Photovoltaic Specialist Conference, 1972.

9. H. E. Nastelin, J. R. Hietanen and F. A. Shirland, ARL 67-0282, December 1967.

10. K. Bogus, D. Huber, S. Mattes, Research Report RVI 1-to-1 (07/7)71 A. E. G. - Telefunken, February 1973.

11. Progress Report NSF/RANN/AER72-03478 A03/PR75/1, May, 1975.

12. Progress Report NSF/RANN/AER72-03478 A04/PR75/4, March 1976.

13. H. W. Brandhorst, Jr., NASA/Lewis Research Center, Communication to Division of Solar Energy, ERDA, 7/16/76.

14. L. C. Burton, B. Baron, T. L. Hench and J. D. Meakin, 19th Annual Electronic Materials Conference, June 1977, To be published.

Table I

CdS/Cu_2S Cells
Short Circuit Current Analysis

	Loss Mechanism (%)								
			Recombination						
Date	Cover Absorption Reflection	Grid Shading	Surface	Bulk	Interface	Grain Boundary	Substrate Absorption	Net Loss %	J_{sc} at AM1 (ma/cm^2)
December 1975	8	19	1	15	5	1	2	42	20
June 1976	8	9	1	15	5	1	2	35	23
March 1977	5	4	1	10	5	1	6	28	25
Present Experiments	5	4	1	7	5	1	6	26	26
Next Generation	4	4	1	5	5	1	2	20	28.0

Maximum Short Circuit Current Under AM1 = 35 ma/cm^2 for Eg of 1.2 eV (Cu_2S)

Table II

CdS/Cu_2S Cells
Design Analysis

Open Circuit Voltage

Date	Junction Area Effect (V)	V_{oc} at AM1
December 1975	-0.06	0.51
June 1976	-0.06	0.51
March 1977	-0.06	0.51
Present Experiments	-0.03	0.54
Next Generation	-0.01	0.56

Fill Factor

Series Resistance Cu_2S	Series Resistance CdS	Field Effect	Net Fill Factor
-0.04	-0.04	-0.03	0.69
-0.02	-0.04	-0.03	0.71
-0.04	-0.01	-0.04	0.71
-0.04	-0.01	-0.04	0.71
-0.03	-0.01	-0.03	0.74

Open Circuit Voltage for Planar CdS/Cu_2S Junction = 0.57 V

Diode Limited Fill Factor = 0.80 (V_{oc} = 0.51)
= 0.81 (V_{oc} = 0.56)

Table III

Key Cell Parameters
Analysis and Actual Efficiencies for AM1

CdS/Cu_2S Cells

Date	Short Circuit Current (ma/cm^2)	Open Circuit Voltage (V)	Fill Factor	Design Efficiency %	Achieved Efficiency %
December 1975	20	0.51	0.69	7.1	6.8
June 1976	23	0.51	0.71	8.2	7.8
March 1977	25	0.51	0.71	9.1	8.6
Present Experiments	26	0.54	0.71	10.0	-
Next Generation	28.0	0.56	0.74	11.6	-

$(CdZn)S/Cu_2S$ Cells

Date	Short Circuit Current (ma/cm^2)	Open Circuit Voltage (V)	Fill Factor	Design Efficiency %	Achieved Efficiency %
Present Experiments	20	0.71	0.77	10.9	-
Next Generation	26	0.74	0.78	15.0	-

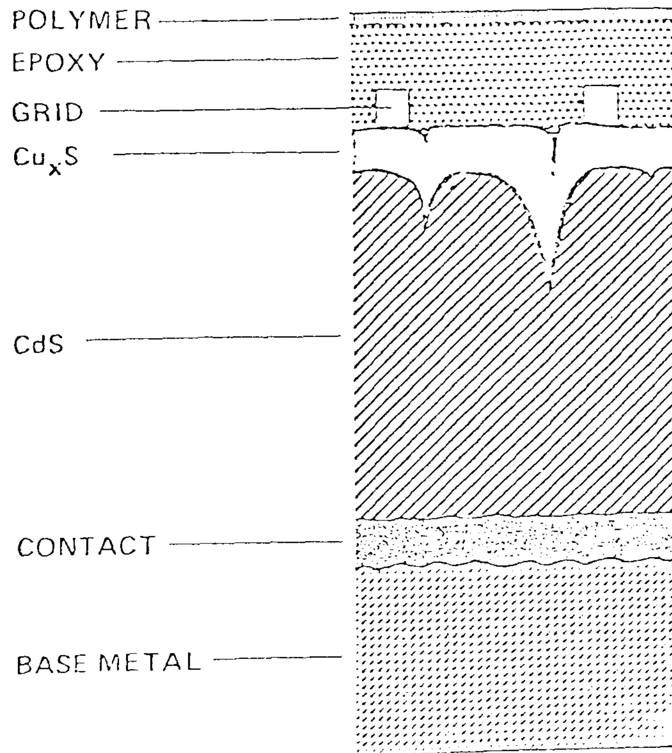

Fig. 1. Traditional CdS/Cu_2S cell structure using pressure bonded front contact.

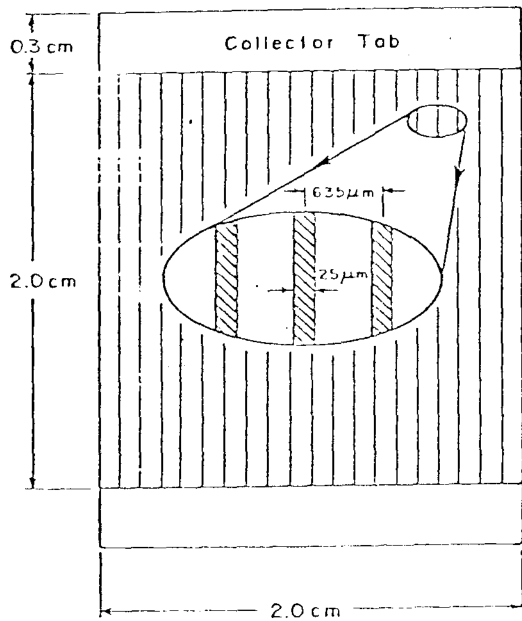

Fig. 2. Geometry of 95% transmission front contact.

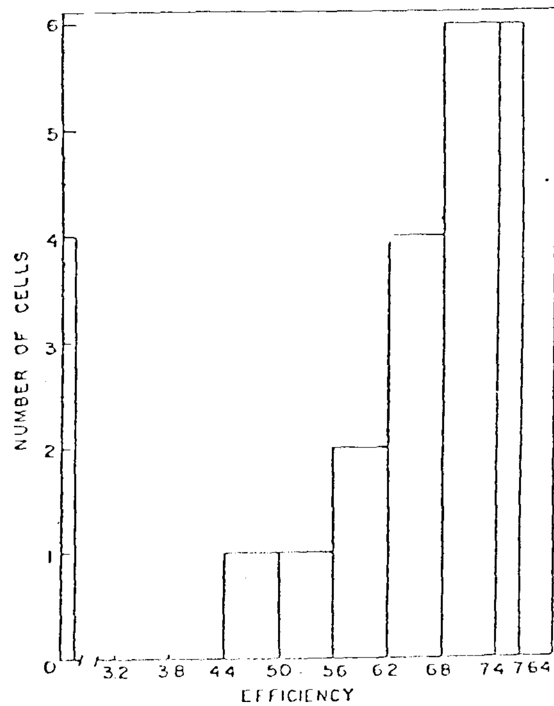

Fig. 3. Distribution of cell efficiencies, June 1976.

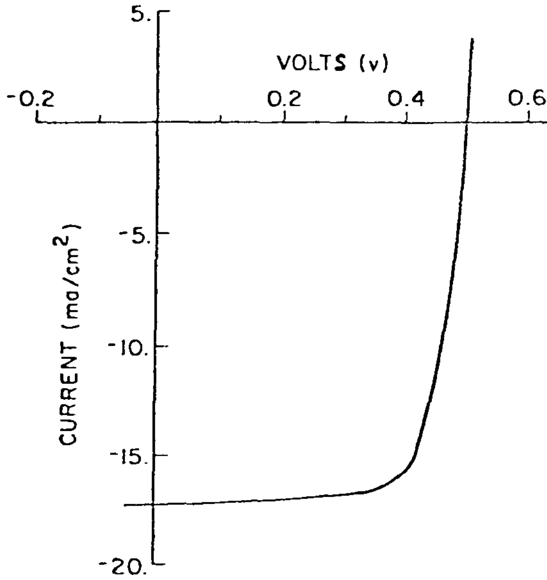

Fig. 4. Collimated sunlight testing for cell 19-1. V_{oc} = 0.50 V, J_{sc} = 17.3 mA/cm^2, FF = 72.6%, efficiency = 7.77%.

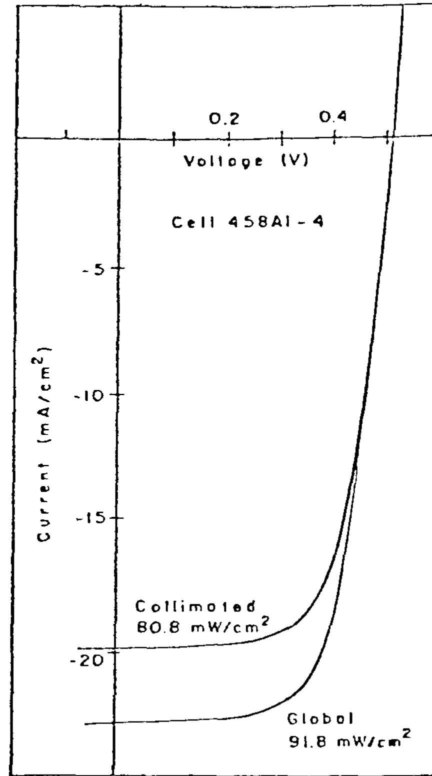

Fig. 5. Sunlight testing of cell 458A1-4, March 1977. The conversion efficiencies in collimated and global sunlight are 8.55 and 8.57%, respectively; the short circuit currents are 25.0 and 25.1 mA/cm^2 prorated to 100 mW/cm^2.

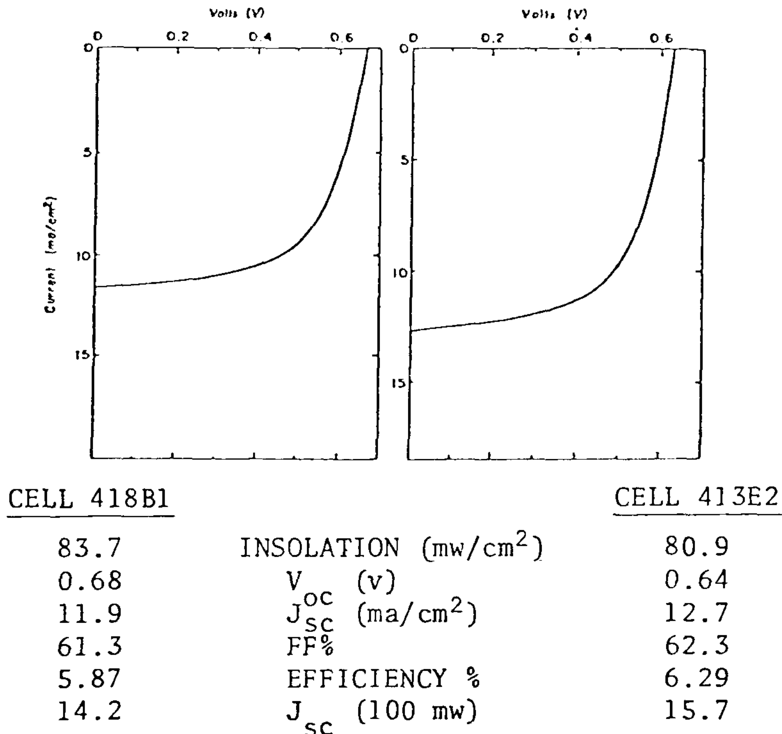

CELL 418B1		CELL 413E2
83.7	INSOLATION (mw/cm^2)	80.9
0.68	V_{oc} (v)	0.64
11.9	J_{sc} (ma/cm^2)	12.7
61.3	FF%	62.3
5.87	EFFICIENCY %	6.29
14.2	J_{sc} (100 mw)	15.7

Fig. 6. Collimated sunlight testing of $(CdZn)S/Cu_2S$ cells 418B1 and 413E2.

Appendix D

FORMATION AND CHARACTERIZATION OF (CdZn)S FILMS AND (CdZn)S/Cu_2S HETEROJUNCTIONS

by

L. C. Burton*, B. Baron, T. L. Hench, J. D. Meakin

Institute of Energy Conversion
University of Delaware
Newark, Delaware 19711

The present status of (CdZn)S/Cu_2S thin film solar cells is reviewed. A new source design has been used to improve the (CdZn)S films. Light reflection loss has been reduced to ∿ 5% by texturing the (CdZn)S surface prior to Cu_2S formation. Using 90% transparent grids, current densities over 16 ma/cm^2 and open circuit voltages over 0.7 volts have been obtained, with a best power conversion efficiency of 6.29%.

key words: solar cells, photovoltaics, thin film solar cells, heterojunctions, solar energy

INTRODUCTION

An energy band diagram for the (CdZn)S/Cu_2S heterojunction is shown in Figure 1. The major anticipated advantage for this junction in comparison to CdS/Cu_2S is a reduction in the height of the conduction band step at the interface as a consequence of improved electron affinity matching. The open circuit voltage is expected to increase by the amount that the electron affinity mismatch decreases.

A substantial number of reports exist in the literature on the formation and characterization of (CdZn)S

* Now at Department of Electrical Engineering, Virginia Polytechnic Institute and State University, Blacksburg, VA 24061

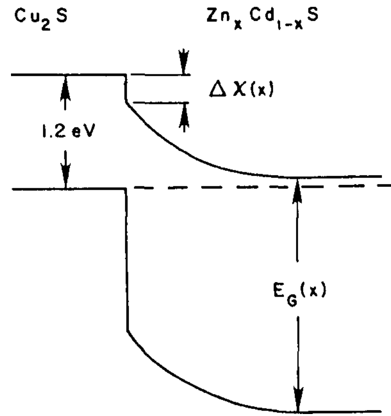

$E_G(x) = (2.42 + 0.49x + 0.43x^2)\,eV$

$E_G(x) = E_G(0) + \Delta E_G$

$\Delta X(x) \sim (0.2 - \Delta E_G)\,eV$

Fig. 1. Energy band diagram for the Cu_2S/ (CdZn)S heterojunction.

crystals (1-4) and films (5-7). This material has also been studied for photovoltaic applications at the University of Delaware (8-10) and elsewhere (11,12). V_{oc} values up to 0.58 v have been reported by other investigators (11) and over 0.7 v has been measured at Delaware (8). We have verified that the increase in V_{oc} is accompanied by the expected increase in barrier height for the reverse current (9,10). The dependence of V_{oc} on zinc content is indicated in Figure 2, with the Cu_2S being formed using techniques previously described (9,10). For cells made to date, the short circuit current densities are less than for CdS cells fabricated under similar conditions.

This paper addresses improvements in (CdZn)S film formation, a reduction in light reflection and grid shading losses, and the present status of (CdZn)S/Cu_2S cells.

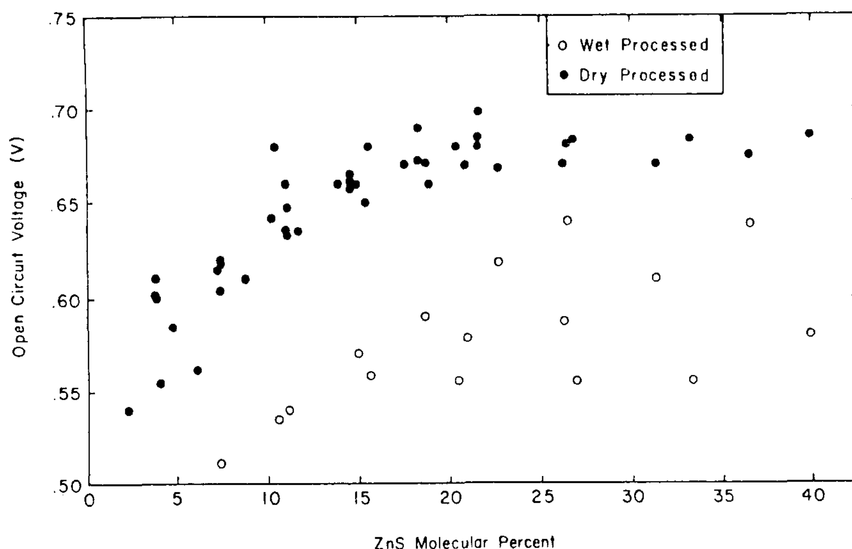

Fig. 2. Dependence of open circuit voltage on zinc content.

Film Deposition

A summary of the evolution of (CdZn)S film deposition techniques used at Delaware is given in Table 1.

The first films made by evaporating powdered (CdZn)S resulted in substantial composition gradients normal to the substrate due to preferential disassociation and evaporation of cadmium and sulfur. Evaporating from independently controlled CdS and ZnS sources gave usable films, but cells were restricted to less than 1 cm in width because of the large lateral composition gradient. More uniform composition was achieved using three identical in-line sources each machined from graphite and contained in a cylindrical tantalum heater. However, to achieve composition control the evaporation rates had to be low, necessitating low source temperatures (< 1100°C). The film resistivity has been shown to increase at low

Table 1

Evolution of (CdZn)S Deposition Techniques

Time Period	2/76-3/76	3/76-8/76	8/76-3/77	3/77-Present
Source Configuration	single source (mixed powder)	2 source	3 source	concentric source
Major Advantages	ease of operation	vertical uniformity	good overall uniformity	control of rate
Major Disadvantages	vertical composition gradient	lateral composition gradient	poor control and repro-ducibility	small vertical gradient

Burton 4

temperatures, and as a consequence the three source method places a lower bound on the reproducibly achievable resistivity. To avoid this problem, a new type of source has since been designed and initial depositions made. A cross-section of this source is shown in Figure 3. The source is machined from graphite and is surrounded by a cylindrical tantalum resistance heater. The filter is quartz wool, contained in a small cylindrical graphite chamber. This concentric design has the following advantages: 1) the single resistanceheater gives better control and reproducibility, 2) relative evaporation rates are determined by the physical parameters of the source (13) and 3) higher source temperatures can be more easily controlled, yielding lower resistivity films.

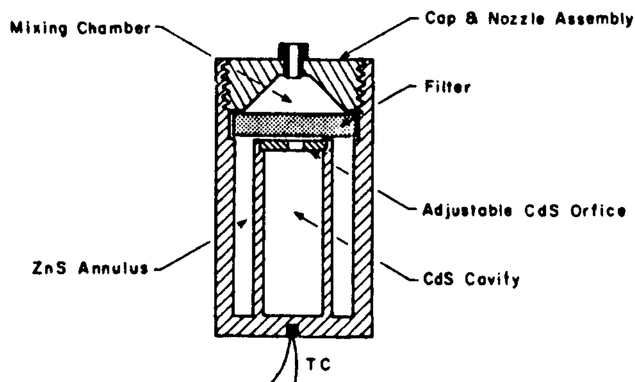

Fig. 3. Cross-section of concentric graphite source currently used for (CdZn)S deposition.

Films in the 0-60% zinc range have been made using this source. Mappings of the lattice parameter by means of x-ray analysis (8) indicate that the lateral uniformity in zinc composition is ±5%. A resistivity of 1 Ω cm has been obtained for a 10% zinc film in comparison to a resistivity of 50-100 Ω cm produced using the multi-source technique. The films produced to date show that 15-20% zinc films with resistivities of 1-10 Ω cm are achievable.

Photovoltaic Junctions

Higher open circuit voltages for the mixed sulfide cells have in general been accompanied by reduced short circuit current (9). The reduced current can result from four major causes: 1) a spike in the conduction band at the interface, 2) reduced absorption coefficient and electron diffusion length in the copper sulfide (14), 3) reflection and grid shading losses at the cell surface and 4) inadequate electric field and mobility in the mixed sulfide depletion region (15).

Referring to Figure 1, the (CdZn)S band gap dependence on composition parameter X was found to be

$$E_G(x) = (2.42 + .49x + .43x^2)\ \text{eV}$$

Assuming that the location of the $Zn_xCd_{1-x}S$ valence band edge is fixed (16), the electron affinity mismatch will decrease by about the same amount that the band gap increases i.e.

$$\Delta X\ (x) \simeq (0.2 - \Delta E_G)\ \text{eV}$$

with an electron affinity mismatch of 0.2 eV between CdS and Cu_2S being assumed (17).

These relations, and open circuit voltage and barrier height measurements, indicate that a conduction band spike should occur in the 25-30% zinc range. For higher zinc content, the current density decrease is caused primarily by the conduction band spike at the interface. (The levelling off of V_{oc} in Figure 2 at ~25% zinc is caused in part by the sharp decrease in short circuit current that occurs). Since our Cu_2S has good stoichiometry ($x \geq 1.996$ in Cu_xS) with resistivity > 0.1 Ω cm, mechanism two, above, is probably not significant. The lower currents for zinc content less than ~25% are thus apparently due to mechanisms not associated with the band spike or bulk properties of the Cu_2S.

The principle remaining mechanisms are related to the reflection and shading losses, and to the electrical properties of the mixed sulfide. For cross comparisons between (CdZn)S and CdS current densities, the optical effects can be made constant by using the same type of grid and surface texturing on both materials. However, it must be verified that the (CdZn)S surface can be textured in a manner similar to CdS, thus reducing reflection loss, before the other loss due to mechanisms in the mixed

sulfide can be identified. With respect to the anti-reflection effects produced by an HCl etch (55% HCl by volume at 60°C), we have shown that the two materials behave in a similar manner. This is indicated in Figure 4 and Table 2. The effect of the etch on the surface topography is seen in the micrographs and is verified by the total reflectivity values given in the table. After the formation of the Cu_2S on the etched surface, the reflectivity is about 5% (4 sec etch - no grid or AR coating present).

Table 2

Total Reflectance Data for CdS and (CdZn)S Surfaces

Sample	% Zn	Before Etch(5)	Etch Time(sec)	After Etch(%)	After Barrier(%)
465	0	25	4	15	5
424	12	21	4	10	5
490-2	21	22	2	12	7
490-4	21	22	4	12	5

The substantial effects of post-gridding heat treatments for mixed sulfide cells are evident in Figs. 5 and 6. In Figure 5 it is seen that I-V parameters (V_{oc}, J_{sc}, fill factor and efficiency) and stability are dependent on heat treatment history, as is the case for the CdS cell. One result of heat treatment that appears different for the two materials relates to the diffusion of copper from the Cu_2S into the n-region. The strong dependence of CdS/Cu_2S junction behavior (both light and dark) on the compensated region in the CdS has been established (15,18).

Junction capacitance values for mixed sulfide cells do not decrease as rapidly with heat treatments as do those for CdS/Cu_2S cells, indicating that copper diffuses more slowly into the mixed sulfide from the Cu_2S. The dependence of light generated current on the compensated (copper diffused) region is expressed by the relation (15)

$$j_L = j_{LO} \frac{\mu F}{\mu F + S}$$

where j_L = light generated current collected
j_{LO} = light generated current with no interface recombination
μ = electron mobility in n-region depletion layer

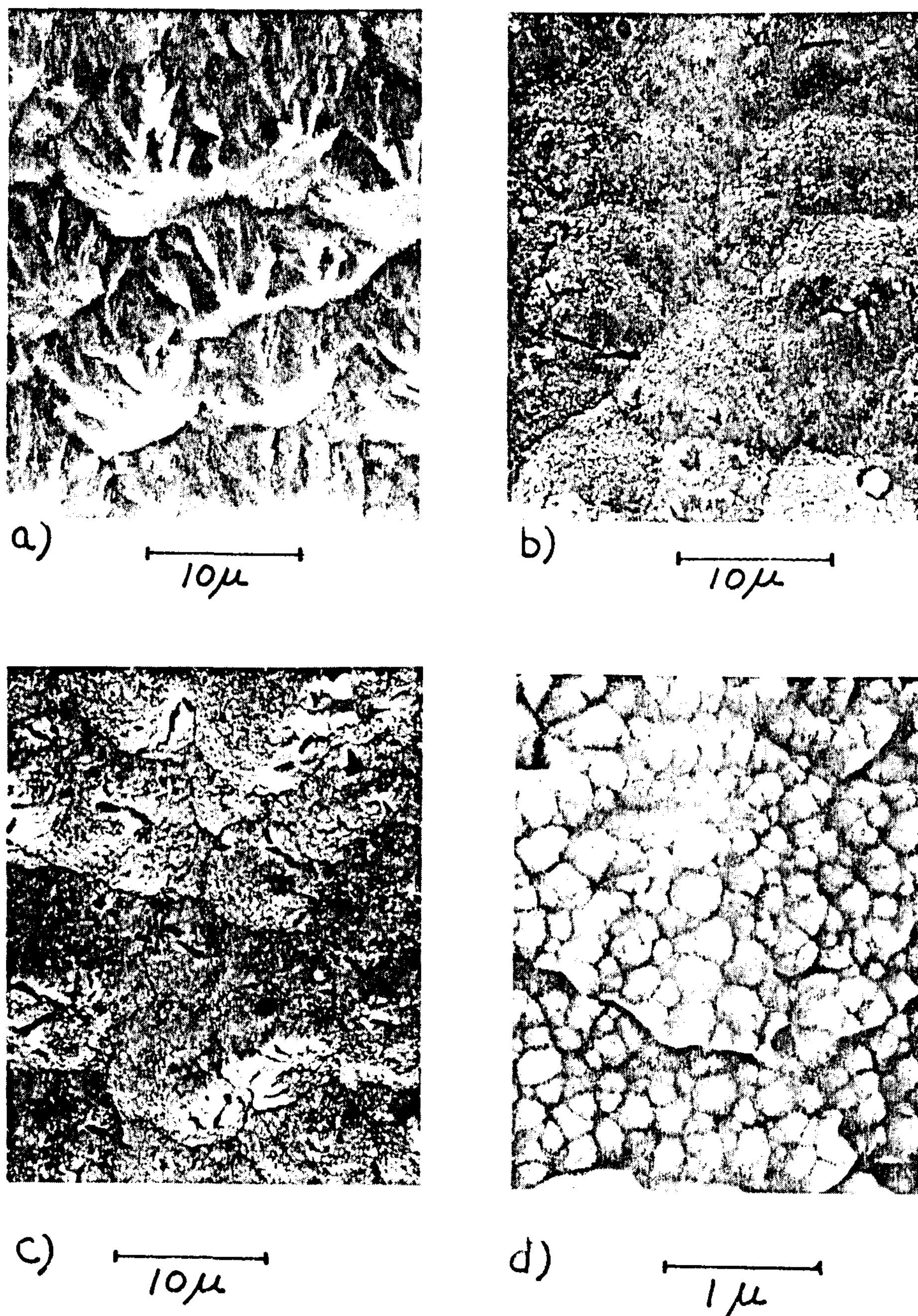

Fig. 4. Scanning electron micrographs of textured (CdZn)S surfaces. Etch times were none (a), 2 sec (b), and 4 sec (c) and (d)

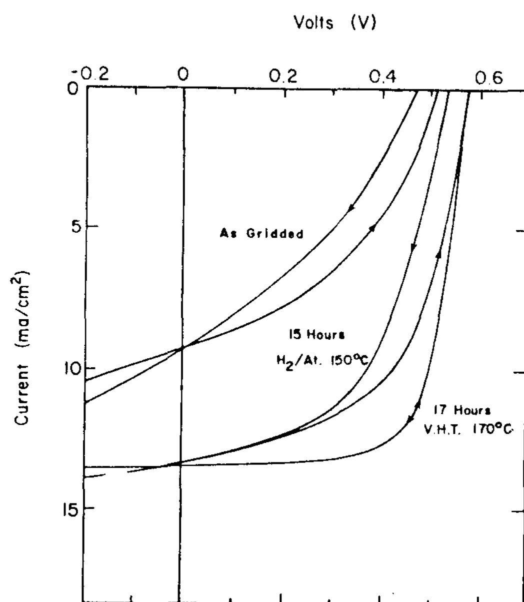

Fig. 5. Effect of heat treatments in 10% hydrogen-90% argon and vacuum (V.H.T.) on response and stability of mixed sulfide cell.

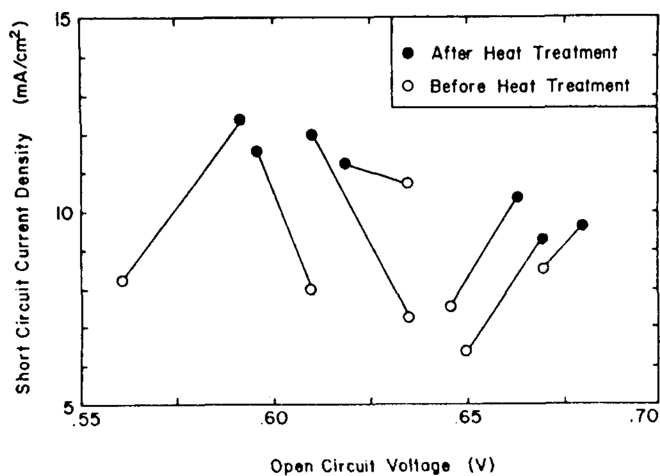

Fig. 6. J_{sc} and V_{oc} changes for several mixed sulfide cells as a consequence of heat treatment in 10% hydrogen-90% argon ambient.

F = electric field at edge of depletion layer
S = interface recombination velocity

j_{LO} is generated almost entirely in the Cu_2S and the question is whether the other terms are significantly different for the mixed sulfide. The electric field is determined by the junction charge profile, which is controlled by the bulk resistivity as modified by copper compensation. Reduced electron mobility could be expected in the mixed sulfide, but the effect on current density is dependent on the relative magnitudes of μF and S. The improved lattice match at the $(CdZn)S/Cu_2S$ interface should reduce the interface state density and hence S, but the electron capture cross section may also be varying. Even for the more extensively studied CdS/Cu_2S junction, these parameters have not been determined to the precision necessary to predict J_{SC} to better than ± 10%, thus the role they play for the mixed sulfide junction remains obscure. The quantitative analysis of current loss mechanisms in the mixed sulfide cell has not yet reached that of the CdS cell, but a major effort is currently underway at Delaware to develope this analysis.

Current-voltage characteristics under actual sunlight for two of the best mixed sulfide cells are given in Figure 7, for V_{OC} values of 0.64 and 0.68 volts. The grids on these cells are only about 90% transparent, and no AR coatings were used. Previous experience shows that application of our best gridding and AR technology to these cells will result in more than 10% improvement in efficiency.

The currents and voltages achieved to date show that the present cell design is capable of power conversion efficiencies over 7.5%. The application of advanced gridding and AR technology developed for the CdS/Cu_2S cell, along with further optimization of the mixed sulfide, should results in further improvements in cell efficiency.

Acknowledgements

This work was supported by NSF-RANN Grant AER 72-03478 and ERDA Grant E(49-18)-2538. We also appreciate the reviewers excellent comments.

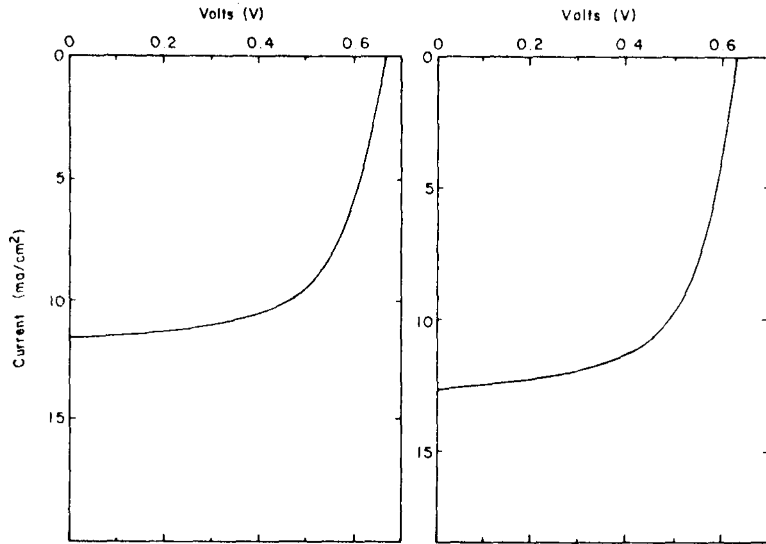

Cell 418B1		Cell 41[illegible]2
83.7	Insolation (mW/cm^2)	80.9
0.68	V_{oc} (v)	0.64
11.9	J_{sc} (mA/cm^2)	12.7
61.3	FF %	62.3
5.87	Efficiency %	6.29
14.2	J_{sc} (100 mW)	15.7

Fig. 7. Current-voltage characteristics for two of the best mixed sulfide cells. Grids are ∿ 90% transparent and cells have no AR coatings.

References

1. D. W. G. Ballantyne and B. Ray, Physica 27, 337 (1961).

2. R. B. Lauer and F. Williams, J. Appl. Phys. 42, 2904 (1971).

3. M. J. Kozielski, J. Crystal Growth 30, 86 (1975).

4. L. G. Suslina, E. I. Panasyuk, S. G. Konnikov and D. L. Fedorov, Sov. Phys. Semicond. 10, 1093 (1976).

5. W. Kane, J. Spratt, L. Hershinger and I. Khan, J. Electrochem. Soc. 113, 136 (1966).

6. D. Bonnet, Phys. Stat. Sol. (a) 11, K135 (1972).

7. D. B. Fraser and H. D. Cook, J. Vac. Sci. Technol. 11, 56 (1974).

8. L. C. Burton and T. L. Hench, Appl. Phys. Lett. 29, 612 (1976).

9. L. C. Burton, B. Baron, W. Devaney, T. L. Hench, S. Lorenz and J. D. Meakin, Proceedings of the 12th IEEE Photovoltaic Specialists Conference, Baton Rouge, LA. (IEEE, New York, 1976), p. 526.

10. Progress Reports NSF/RANN/AER72-03478 A04 FR76, E(49-18)-2538 PR76/1, E(49-18)-2538 PR 76/2, Institute of Energy Conversion, University of Delaware (1977).

11. W. Palz, J. Besson, T. Nguyen Duy, and J. Vedel, Proceedings of the 10th IEEE Photovoltaic Specialists Conference, Palo Alto, CA (IEEE, New York, 1973).

12. T. M. Peterson, Ph. D. Thesis (Lawrence Berkely Laboratory, University of California at Berkely, 1975).

13. D. Beecham, Rev. Sci. Instrum. 41, 1654 (1970).

14. L. C. Burton and H. M. Windawi, J. Appl. Phys. 47, 4621 (1976).

15. A. Rothwarf, Technical Report NSF/RANN/AER 72-03478 A04/TR76/1, Institute of Energy Conversion, University of Delaware (1976).

16. J. O. McCaldin, T. C. McGill and C. A. Mead, J. Vac. Sci. Technol. 13, 802 (1976).

17. A. Rothwarf and A. M. Barnett, IEEE Transactions on Electron Devices ED-24, 381 (1977).

18. L. R. Shiozawa, F. Augustine, G. A. Sullivan, J. M. Smith III and W. R. Cook, Jr., Clevite Final Report No. ARl 69-0155 (Clevite Corporation, Cleveland, 1969).

Appendix E

Reports and Publications

1. Progress Reports

   E(49-18)-2538 PR 76/1
   E(49-18)-2538 PR 76/2
   E(49-18)-2538 PR 77/1

2. Publications

A. M. Barnett, A. Rothwarf, "Advances in the Development of Efficient Thin Film CdS/Cu_2S Solar Cells," 12th IEEE Photovoltaic Specialists Conference, p. 544-546, 1976.

L. Burton, H. Windawi, "Thermally Induced Changes in Cu_xS Films and Effect on CdS/Cu_xS Solar Cell Response," Journal of Applied Physics, Vol. 47, No. 10, pp. 4621-4626, October 1976.

L. Burton, B. Baron, W. Devaney, T. Hench, S. Lorenz, J. D. Meakin, "Studies Related to $Zn_xCd_{1-x}S$/Cu_2S Solar Cells," 12th IEEE Photovoltaic Specialists Conference, pp. 526-528, 1976.

L. Burton, T. Hench, "$Zn_xCd_{1-x}S$ Films for Use in Heterojunction Solar Cells," Appl. Phys. Lett. 29, 612, 1976.

W. Devaney, S. Lorenz, J. D. Meakin, "Spectral Response Measurements with White Light Bias," NASA Second Solar Simulation Workshop, pp. 385-391, 1976.

J. D. Meakin, B. Baron, K. W. Böer, L. Burton, W. Devaney, H. Hadley, J. Phillips, A. Rothwarf, G. Storti, W. Tseng, "CdS/Cu_2S Solar Cells, A Low Cost Thin Film Crystalline Photovoltaic Device for Terrestrial Applications," Proc. Sharing the Sun, Winnipeg, 1976.

A. Rothwarf, "Crystallite Size Considerations in Polycrystalline Solar Cells," 12th IEEE Photovoltaic Specialists Conference, pp. 488-495, 1976.

L. C. Burton, T. Hench, G. Storti, G. Haacke, "CdS/Cu_2S Solar Cells Fabricated on Cd_2SnO_4-Silica Substrates, J. Electrochemical Society, 123, 1741-1744, 1976.

G. Storti, J. Culik, "The Relationships Between Preparation Parameters, Operating Characteristics and Physical Processes in Cu_2S/CdS Thin Film Solar Cells," 12th IEEE Photovoltaic Specialists Conference, pp. 462-465, 1976.

☆U.S. GOVERNMENT PRINTING OFFICE: 1978-740-094/1445